

University of Montana

ScholarWorks at University of Montana

Graduate Student Theses, Dissertations, &
Professional Papers

Graduate School

1982

Mylonitic fabric development through the east flank of the Bitterroot dome Montana

Peter Watson Rankin
The University of Montana

Follow this and additional works at: <https://scholarworks.umt.edu/etd>

Let us know how access to this document benefits you.

Recommended Citation

Rankin, Peter Watson, "Mylonitic fabric development through the east flank of the Bitterroot dome Montana" (1982). *Graduate Student Theses, Dissertations, & Professional Papers*. 7596.
<https://scholarworks.umt.edu/etd/7596>

This Thesis is brought to you for free and open access by the Graduate School at ScholarWorks at University of Montana. It has been accepted for inclusion in Graduate Student Theses, Dissertations, & Professional Papers by an authorized administrator of ScholarWorks at University of Montana. For more information, please contact scholarworks@mso.umt.edu.

448-1

COPYRIGHT ACT OF 1976

THIS IS AN UNPUBLISHED MANUSCRIPT IN WHICH COPYRIGHT SUBSISTS. ANY FURTHER REPRINTING OF ITS CONTENTS MUST BE APPROVED BY THE AUTHOR.

MANSFIELD LIBRARY
UNIVERSITY OF MONTANA
DATE: 1982

MYLONITIC FABRIC DEVELOPMENT THROUGH
THE EAST FLANK OF THE BITTERROOT DOME, MONTANA

by

Peter Watson Rankin

B.S., University of Washington, 1976


Presented in partial fulfillment of the
requirements for the degree of

Master of Science

UNIVERSITY OF MONTANA

1982

Approved by:


Chairman, Board of Examiners


Dean, Graduate School

3-19-82
Date

UMI Number: EP38397

All rights reserved

INFORMATION TO ALL USERS

The quality of this reproduction is dependent upon the quality of the copy submitted.

In the unlikely event that the author did not send a complete manuscript and there are missing pages, these will be noted. Also, if material had to be removed, a note will indicate the deletion.



UMI EP38397

Published by ProQuest LLC (2013). Copyright in the Dissertation held by the Author.

Microform Edition © ProQuest LLC.

All rights reserved. This work is protected against unauthorized copying under Title 17, United States Code



ProQuest LLC.
789 East Eisenhower Parkway
P.O. Box 1346
Ann Arbor, MI 48106 - 1346

ABSTRACT

Rankin, Peter Watson, M.S., Winter, 1982

Geology

Mylonitic Fabric Development Through the East Flank of the Bitterroot Dome

Director: Donald W. Hyndman



A gently-dipping, 100 km-long mylonitic shear zone, up to 1.6 km-thick, forms the east flank of the Bitterroot dome and is a major zone of detachment separating the Idaho batholith infrastructure from its eastward displaced suprastructure or Sapphire tectonic block. The Bitterroot dome and the average 20° angle of dip of the east flank are the result of isostatic recovery after detachment.

Mylonite gneisses within the zone were derived mostly from, and structurally overlie nearly undeformed granitic rocks of the Idaho batholith. The degree of deformation, evidenced by intragranular recrystallization, strain and rupture, and intergranular generation of matrix material, increases upward through the zone and rocks progressively developed stronger foliation and lineation during development of the mylonitic fabric. Most of the fabric characteristics evolved under deep-seated ductile conditions. However, within the upper portion of the zone and crossing the dome, east-trending mineral streak and "slickenside" striae occur on closely spaced shear surfaces and must have formed late in the deformation sequence under shallower more-brittle conditions as the Sapphire block moved off of the infrastructure.

Quartz [0001] and poles to biotite {001} show nearly random orientation in nonmylonitic samples. Quartz [0001] in mylonitic samples form great circle-girdle patterns approximately normal to lineation, with double or single maxima lying close to or symmetrically about the foliation. Poles to biotite {001} display strong single maxima, normal to foliation, within a weak great-circle girdle parallel to lineation.

Fabric symmetry derived from structural analysis of mesoscopic foliation and lineation, and microscopic orientation of quartz [0001] and poles to biotite {001}, is orthorhombic. Thus, the type of strain, and the plane and line of translation represented by foliation and lineation, respectively, through the zone could be determined directly from the fabric, but not the direction or magnitude. Under ductile conditions, inhomogeneous pure shear likely dominated initially, gradually gave way to inhomogeneous simple shear which, as physical conditions changed, led ultimately to brittle rupture and further detachment on individual shear surfaces.

ACKNOWLEDGMENTS

I would like to thank my thesis committee members, David M. Fountain and John D. Scott for their assistance during the course of this study, and especially my thesis chairman Don W. Hyndman who inspired and encouraged my interest in the subjects of this thesis. Steve Balogh provided invaluable help in preparing and staining oriented thin sections and Shirley Pettersen not only did all of the typing, but provided great moral support and humor which I truly appreciate.

My parents, as always, offered their love and understanding, and David, Gil, Bud and Carey were close cohorts in crime and truth.

I would like to express my special thanks to Lorraine, who with Cedar, Otis and Omar shared some of the most pleasant days of my time here.

TABLE OF CONTENTS

	Page
ABSTRACT	ii
ACKNOWLEDGMENTS	iii
LIST OF FIGURES	vi
LIST OF PLATES	viii
CHAPTER	
I. INTRODUCTION	1
General Statement	1
Present Study	2
Previous Work	3
Location and Access	3
II. REGIONAL SETTING	7
General Geology	7
Bitterroot Dome - Sapphire Tectonic Block	8
III. MESOSCOPIC STRUCTURAL GEOLOGY AND FIELD RELATIONSHIPS	13
General Statement	13
Map Units	14
Foliation	16
Lineation	19
IV. DESCRIPTIVE PETROGRAPHY	21
General Statement	21
Nonmylonitic Interior	21
Weakly Mylonitic Zone	26
Strongly Mylonitic Zone	27

CHAPTER	Page
Black Mylonite	29
White Mylonite	37
Black Dikes	37
Chemical Similarities	37
V. DESCRIPTIVE MICROSCOPIC STRUCTURAL ANALYSIS	39
General Statement	39
Quartz C-axis Orientation	40
Deformation Lamellae	47
Biotite Orientation	49
Fabric Symmetry from Microscopic and Mesoscopic Elements	51
VI. DYNAMIC INTERPRETATION	54
General Statement	54
Physical Conditions in the Mylonitic Zone	54
Fabric Development	55
Implications of Preferred Orientation and Symmetry	62
Movement Picture	64
VII. COMPARISON WITH SIMILAR COMPLEXES AND MYLONITE ZONES	66
VIII. CONCLUSIONS	70
REFERENCES CITED	73
APPENDIX 1: Thin Section Analyses	77
APPENDIX 2: Chemistry and Chemical Variation Diagram	79

LIST OF FIGURES

Figure	Page
1. Thesis area location map	4
2. Previous work map	6
3. Regional geologic map; Bitterroot dome, mylonitic shear zone and Sapphire tectonic block	10
4. West-to-east cross section through the northern Idaho batholith and Sapphire tectonic block	11
5. Sketch of small asymmetric folds	13
6. Geologic map of the field area	15
7. Cross sections A-A' and B-B' with sample locations . . .	17
8. Orientation diagram - poles to foliation	18
9. Orientation diagram - mica streak and "slickenside" lineations	18
10. Sketch of typical sample - SMZ	20
11. Thin section modes on IUGS classification diagram . . .	22
12-20. Orientation diagrams for quartz [0001]	
12. NM1 Sample C-10b	42
13. NM1 Sample RL-1b	43
14. WMZ Sample C-11b	43
15. WMZ Sample RL-13b	44
16. WMZ Sample RL-19b	44
17. SMZ Sample RL-B	45
18. SMZ Sample C-4b	45
19. SMZ Sample RL-25b (black mylonite)	46
20. SMZ Sample RL-30b (white mylonite)	46

LIST OF FIGURES (cont.)

FIGURE	Page
21. Orientation of "Boehm" and deformation lamellae	47
22-24. Orientation diagrams for poles to biotite {001}	
22. NM1 sample RL-1b	50
23. WMZ sample RL-13a	50
24. SMZ sample RL-A	51
25. Diagram displaying combined symmetry elements	52
26. Paragenetic sequence for minerals in the mylonitic zone .	56
27. Summary of fabric development	57

LIST OF PLATES

Plate	Page
1. Mesoscopic fabric of nonmylonitic interior sample C-10	24
2. Photomicrograph of nonmylonitic interior sample BL-3 .	24
3. Typical outcrop of weakly mylonitic zone mylonite gneiss	31
4. Photomicrograph of weakly mylonitic zone fabric; sample RL-13a	31
5. Photomicrograph of weakly mylonitic zone fabric; sample RL-13	32
6. Outcrop of strongly mylonitic zone mylonite gneiss and black mylonite	32
7. Sample from the strongly mylonitic zone mylonite gneiss and white mylonite	33
8. Photomicrograph of strongly mylonitic sample RL-29a .	33
9. Photomicrograph of strongly mylonitic sample C-4a with offset plagioclase grain along shear surface . .	34
10. Photomicrograph of strongly mylonitic sample RL-25a displaying shear-step texture	34
11. Photomicrograph of strongly mylonitic sample GS-1a. Pulled apart plagioclase	35
12. Photomicrograph of strongly mylonitic sample RL-30b. Deformation twins in strained plagioclase	35
13. Photomicrograph of strongly mylonitic sample C-4b. Nearly euhedral, broken and annealed plagioclase included in relatively undeformed K-feldspar megacryst	36
14. Photomicrograph of strongly mylonitic black mylonite sample C-9a. Plagioclase augen breaking up into smaller grains	36
15. Photomicrograph of deformation lamellae in quartz, sample RL-19	48

CHAPTER I

INTRODUCTION

General Statement

The straight, north-trending, gently-dipping front of the Bitterroot Mountains in Montana has attracted the attention of geologists at least since 1904, when Lindgren (1904) first mapped the area.

What is now recognized as a distinct stratiform zone of mylonitic shearing, 100 km long and up to 1.6 km thick, forms this front and gives it the uniform slope flanking the rugged interior of the Bitterroot Range to the west. Numerous theories evolved throughout the years to explain the origin of this zone and although detailed petrographic study has left little doubt about its "mylonitic" nature, it was regional work that revealed its probable role in the overall tectonic picture of the area. Certainly with more data at hand, and perhaps a broader perspective than earlier workers, Hyndman and others (1975) proposed that this zone of mylonitic shearing or zone of cataclasis (Chase, 1973) was a major zone of detachment separating the Idaho batholith infrastructure from its displaced suprastructure or Sapphire tectonic block.

A similar situation exists for more than 25 "metamorphic core complexes" (Coney, 1980) intermittently exposed from southern British Columbia to northwestern Mexico, and although they differ somewhat in age and detail, all possess at least three common elements: 1) a

high-grade infrastructure, consisting of sillimanite-zone regional metamorphic rocks and/or granitic plutons displaying flowage under high-temperature, deep-seated ductile conditions, 2) an overlying or adjacent unmetamorphosed to low-grade suprastructure, displaying open folds and faults developed under shallow brittle conditions, and 3) an intervening gently-dipping lineated and foliated mylonitic shear zone from several meters to over a kilometer thick, commonly exhibiting characteristics of both ductile and brittle deformation.

The mylonitic rocks along the front and the underlying nonmylonitic rocks are the subject of this study and any theory regarding their origin must account for the mesoscopic and microscopic fabric characteristics within the zone of its position relative to adjacent terranes of divergent rock type, metamorphic grade, and structural style.

Present Study

This study involved mapping and sampling sections through the mylonitic zone into nonmylonitic rocks of the Idaho batholith. In addition to mapping and recording lithologic and structural characteristics, 50 oriented and 8 unoriented samples were collected. Forty thin sections from selected oriented samples were cut at various orientations to provide information on fabric characteristics. Nine sections were analyzed for quartz orientation and three for biotite orientation on a four-axis universal stage microscope. Most of the field work was conducted during the fall of 1979.

This study was designed to provide information on fabric development and mineral orientation in mylonitic rocks derived from essentially isotropic rocks of the Idaho batholith. The mesoscopic fabric, its microstructures and symmetry are critical elements to any theory for the mylonitic zone.

Location and Access

The study area is in west-central Ravalli County, Montana, west and southwest of the town of Hamilton within the Hamilton North, Hamilton South, Printz Ridge and Ward Mountain 7½ minute quadrangles (see Fig. 1). It is approximately 160 square kilometers in area. Elevation varies from 1097 meters in the Bitterroot Valley to a maximum of 2780 meters at Ward Mountain.

County, private and U.S.F.S. roads provide access to trails starting at the eastern front of the Bitterroot Range and lead westward up drainages and in some cases ridges. In this area the Bitterroots are cut by a number of east-trending, steep-walled glaciated valleys providing excellent rock exposures on valley walls and ridge crests.

Previous Work

Lindgren (1904) first described the mylonitic zone and concluded that a uniform dislocation of great extent had occurred along the east slope of the Bitterroot Range. Except for Langton (1935) and Ross (1952), other regional studies such as Chase (1973, 1977), Clark (1979), Hyndman (1977, 1980), Hyndman and others (1975), and Hyndman and Williams (1977) also at least agree on the "mylonitic" character of the Bitterroot Front.

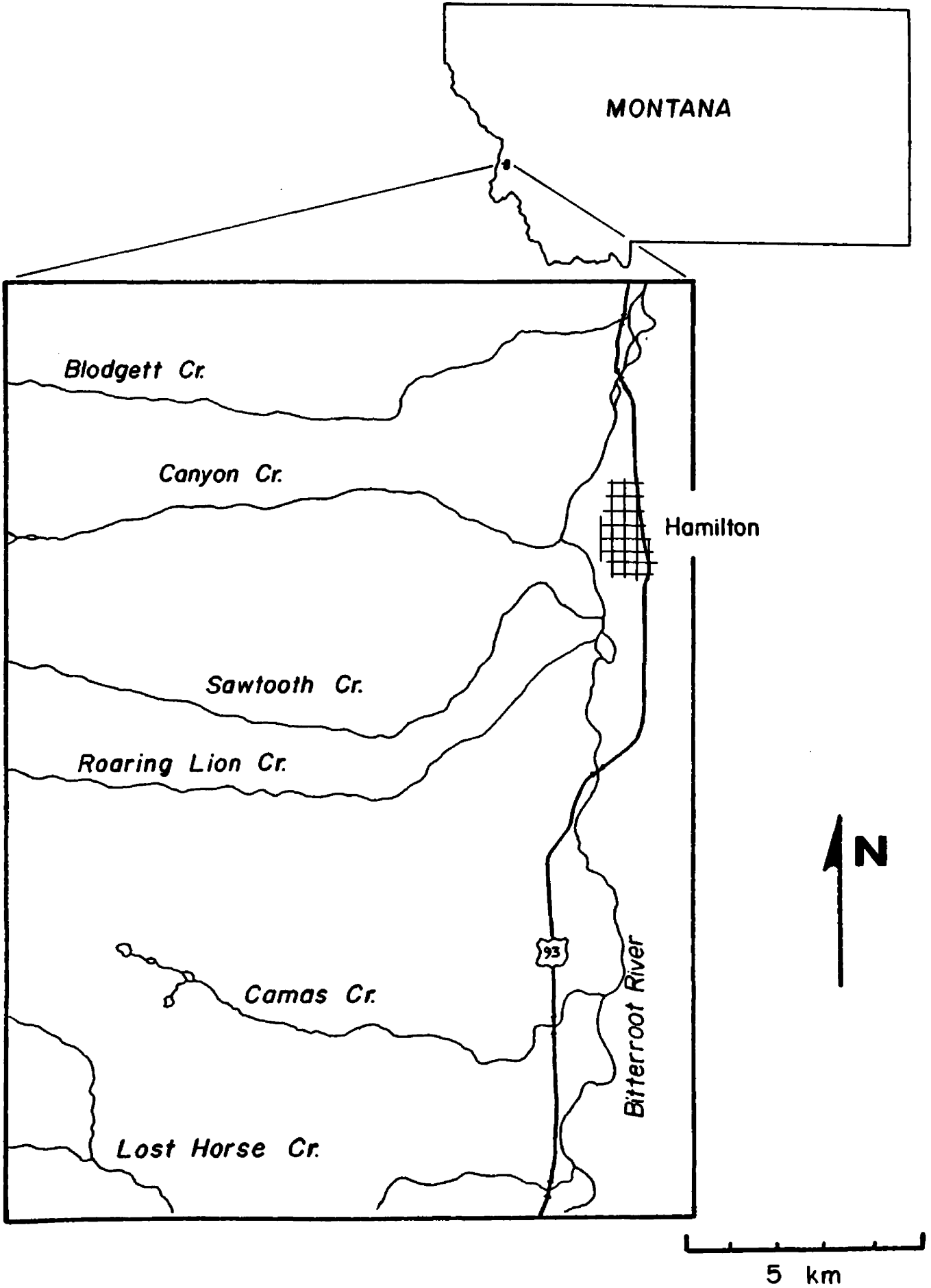


Figure 1. Thesis area location map.

Published studies (Berg, 1968; Chase, 1973; Cheney, 1975; Greenwood and Morrison, 1973; Jens, 1974; Larson and Schmidt, 1958; Nold, 1974; Wehrenberg, 1972; Winegar, 1973, U.S.F.S. open file report) and unpublished theses (Anderson, 1959; Chase, 1961; Groff, 1954; Hall, 1968; Leischer, 1959; White, 1969; Williams, 1975) describe in detail specific areas along the Bitterroot Front and northeast border zone of the Idaho batholith. Figure 2 shows the location of some of these studies. Hyndman and others (1975) and Chase and others (1978) report radiometric ages between about 60 and 90 million years for the Idaho batholith.

Most previous work was either conducted on a larger scale or involved areas to the north of this study area and include rocks besides those derived from the Idaho batholith.

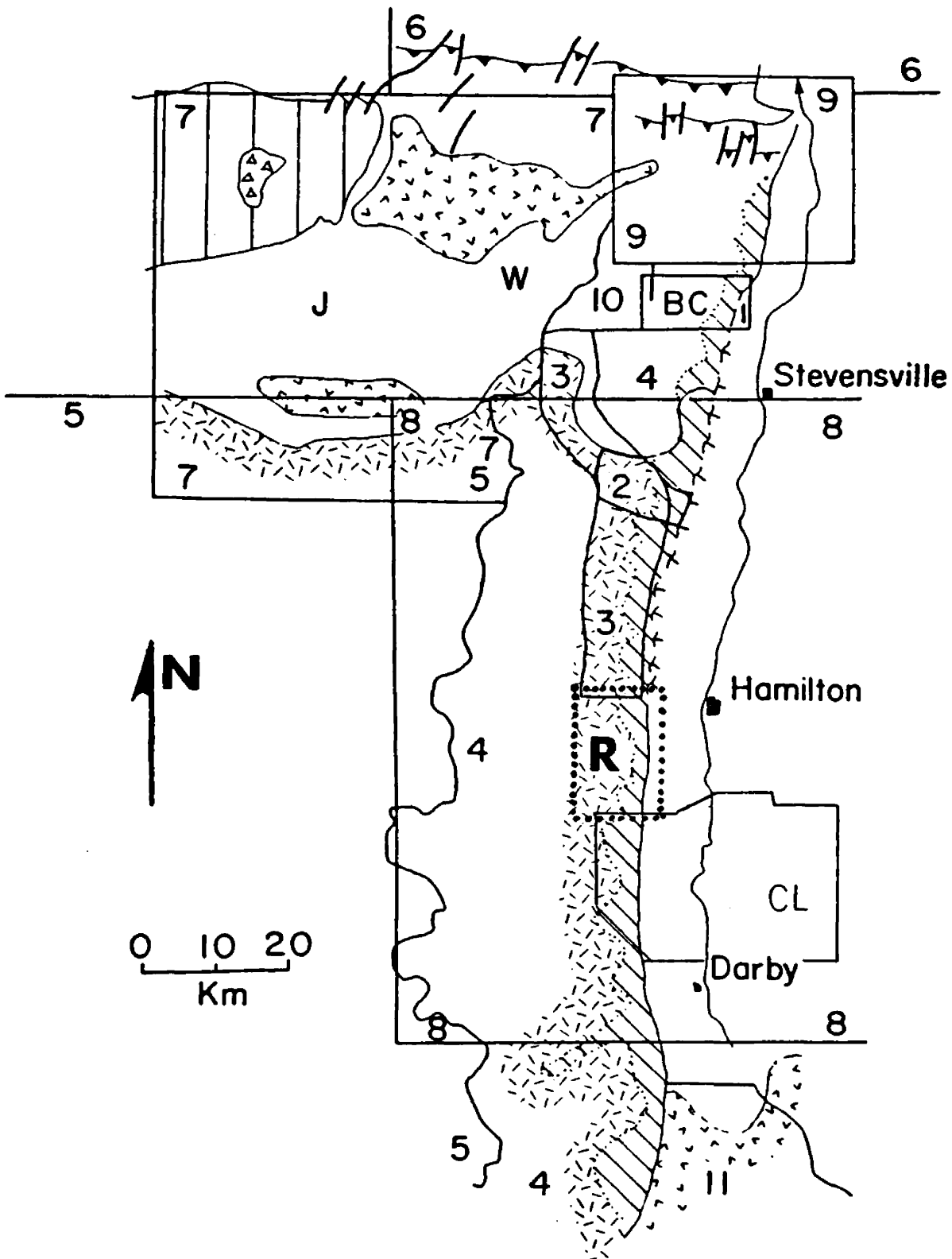


Figure 2. Previous work map; 1 = Anderson (1959), 2 = Chase (1961), 3 = Chase (1973), 4 = Chase (ms.), 5 = Greenwood and Morrison (1973), 6 = Hall (1968), 7 = Nold (1974), 8 = Ross (1952), 9 = Wehrenberg (1972), 10 - Williams (1975), 11 - Winegar (U.S.F.S. Open File Report). Locations of specific studies are B = Berg (1968), C = Cheney (1974), CL = Clark (1979), J = Jens (1974), R = Rankin (present study area), W = White (1969). (Adapted from Chase, 1977)

CHAPTER II

REGIONAL SETTING

General Geology

West-central Montana and the adjacent portion of Idaho is dominated physiographically by the rugged Bitterroot Range in the west (Clearwater Mountains in Idaho), the intermontane north-trending Bitterroot River Valley, and the more subdued Sapphire and Flint Creek ranges to the east. As might be expected, the geography reflects the geologic-tectonic picture of the region.

The Bitterroot Range can be divided geologically into two sectors (Chase, 1973). The northern one-third of the range contains regionally metamorphosed gneiss, schist, amphibolite, and small anorthosite bodies. This area has undergone polyphase deformation, up to sillimanite-orthoclase-grade metamorphism and intrusion by tabular igneous bodies. The gneiss, schist, and amphibolite probably represent a high-grade equivalent of the lower Precambrian Belt Supergroup, namely the Prichard Formation with its common mafic sills and dikes. The anorthosite described by Berg (1968) may be a part of pre-Belt basement. The southern two-thirds of the range contains rocks ranging in composition and structure from foliated quartz diorite to massive megacryst-bearing granite (Chase, 1977; IUGS classification, Streckeisen, 1973) of the eastern portion of the Bitterroot lobe of the Idaho batholith.

The 100 km-long east-dipping mylonitic zone forming the straight gentle slope of the Bitterroot Front imposes a shear foliation on both the batholithic and metamorphic rocks.

Tertiary volcanic rocks and sediments in the Bitterroot River Valley are overlain by glacial deposits along the east-draining tributaries of the Bitterroot Range, and Lake Missoula sediments along the western flank of the Sapphire Mountains (Clark, 1979). Locally, igneous, metamorphic, and Belt rocks crop out along the floor of the valley.

The Sapphire Range consists primarily of Precambrian upper Belt sedimentary rocks belonging to the Missoula Group and underlying Wallace Formation. Metamorphism is generally low-grade chlorite zone except in the south and southwest where grade increases to lower, and locally upper, amphibolite facies (Hyndman, 1980). High-grade rocks mapped by Clark (1979) may be lower Belt to pre-Belt and possibly correlative with rocks in the northern Bitterroots. Sizable granitic bodies occur in the range as well as at least one small alkali pyroxenite complex described by Lelek (1979).

The Flint Creek Range contains similar upper-Belt Missoula Group rocks in addition to nearly a complete section of overlying Paleozoic-Mesozoic sedimentary rocks in the eastern part of the range (Hyndman, 1980).

Bitterroot Dome-Sapphire Tectonic Block

Lindgren (1904) and virtually all workers since, recognized that the Bitterroot Range rose with respect to the Sapphire Range. Hyndman

and others (1975) proposed that the Sapphire and Flint Creek ranges comprised a distinct structural block or "Sapphire tectonic block" that slid more than 25 km eastward off the Bitterroot infrastructure or Bitterroot dome (Talbot and Chase, 1973) with the intervening mylonitic zone forming the detachment surface (see Figs. 3 and 4).

Hyndman (1980) modified the picture slightly, proposing 60 km of eastward movement with the easternmost 20 km of the Flint Creek Range being bulldozed ahead of the moving block. The north-trending 100 km by 60 km elliptical Bitterroot dome is matched in its dimensions by the 100 km by 70 km Sapphire tectonic block.

The dome is asymmetric with respect to fabric, in that shear foliation and mineral streak and "slickenside" lineation are strongest in the mylonitic zone and fade downward and westward across the top of the dome. The penetrative "slickenside" lineation crosses the entire dome and maintains an almost constant east-southeast trending orientation even where the foliation dips south at the southern end of the dome. This suggests that the dome was not present prior to offloading of the Sapphire block and that unidirectional movement occurred off the entire unloaded area. The dome, and the present average 20° angle dip of the mylonitic zone, presumably resulted from isostatic recovery.

Formation of the mylonitic zone by detachment of the Sapphire tectonic block occurred during the last stages of consolidation of the Idaho batholith (Hyndman, 1980). Based primarily on the late Cretaceous age of thrusting in the eastern part of the block, detachment occurred 75-80 m.y. ago (Hyndman, 1980). Radiometric ages for the batholith range

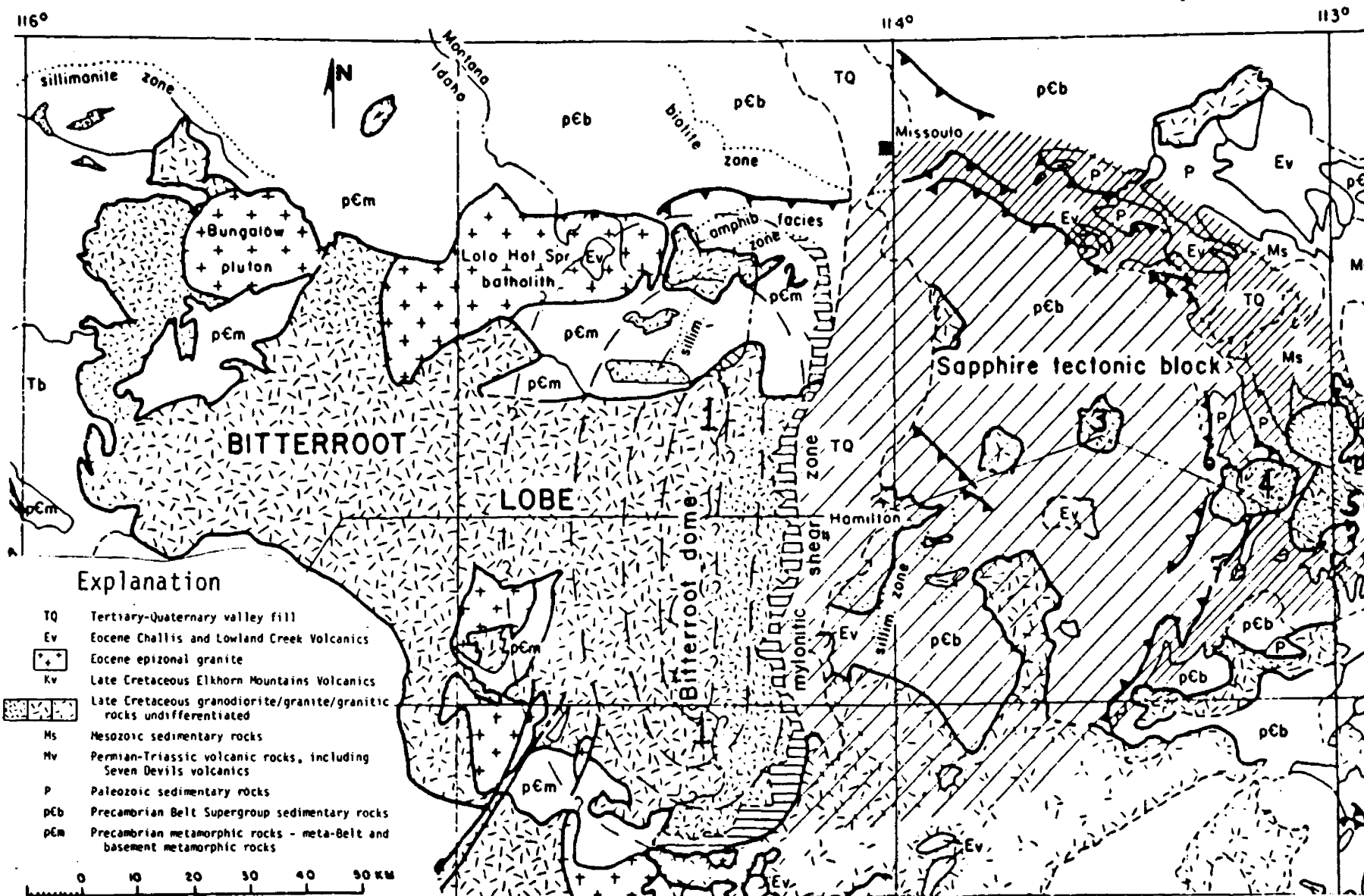


Figure 3. Regional geologic map showing relationship between the Bitterroot dome, mylonitic shear zone, and Sapphire tectonic block. (Adapted from Hyndman, 1980)

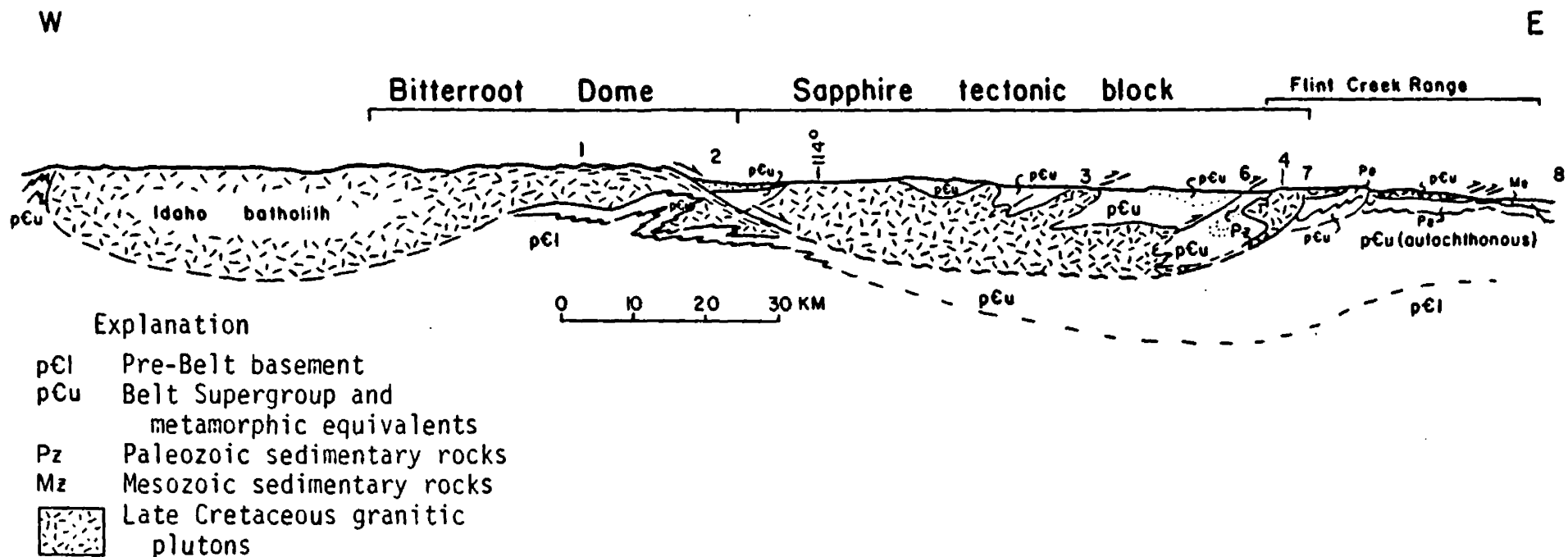


Figure 4. West-to-east cross section through the northern Idaho batholith and Sapphire tectonic block. 1 - crest of Bitterroot dome at Idaho-Montana border, 2 = mylonitic shear zone, west side Bitterroot Valley, 3 = Miner's Gulch stock, 4 = Philipsburg batholith, 5 = Racetrack Creek pluton, 6 = Philipsburg thrust, 7 = Georgetown thrust. 8 = Deer Lodge Valley. (Adapted from Hyndman, 1980).

between about 55 and 90 million years (Hyndman and others, 1975; Chase and others, 1978; Chase, in press; Hyndman personal communication, 1981).

Superposition of brittle shear features (ie. shear surfaces containing penetrative "slickensides") on ductile mylonitic fabrics in the mylonitic zone indicates that conditions changed dramatically during the evolution of the zone. Presumably, as the block was unloaded the underlying rocks approached the surface and the style of deformation (and resulting fabric) changed from deep-seated plastic flow to shallow brittle shearing.

The thickness of the Sapphire tectonic block is estimated by Hyndman (1980) to be on the order of 17 km. This figure is derived by estimating the combined stratigraphic thickness of Belt rocks within the block, and by determining the pressure-temperature conditions from mineral assemblages found in and below the mylonitic zone.

CHAPTER III

MESOSCOPIC STRUCTURAL GEOLOGY AND FIELD RELATIONSHIPS

General Statement

The structural geology of the field area is relatively straightforward. Mylonitic foliation and lineation are by far the most important mesoscopic and macroscopic structural elements. Unlike the northern portion of the dome where the mylonitic zone cuts complexly folded paragneiss and schist below the floor of the batholith (Chase, 1973), folds of any magnitude are rare within or non-existent below the mylonitic zone bordering relatively undeformed batholithic rocks. The few folds encountered in the zone are generally small, affect only thin layers, and from their asymmetry suggest a downdip sense of movement (see Fig. 5). Aside from perhaps a major fault mapped by Lindgren (1904), Chase (1973) and Clark (1979), paralleling the base of the Bitterroot

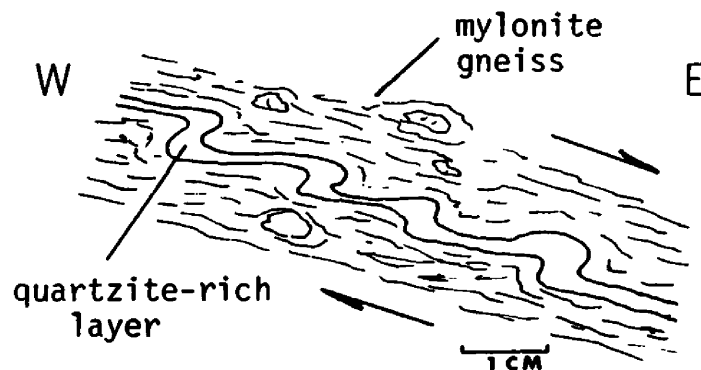


Figure 5. Sketch of late, asymmetric folds in the mylonitic zone showing downdip sense of movement.




front and offsetting the mylonitic zone, only a few near-vertical north-trending slickensided or chloritic joint surfaces were observed. Although offset appeared minimal, these may have resulted from late rise of the dome (Hyndman, 1980, p. 44) or Tertiary events unrelated to the dome. Foliation joints along shear planes in the zone give the Bitterroot front its characteristic stratified appearance. Strike joints commonly filled with quartz, epidote or chlorite are common and offer evidence of extension approximately perpendicular to the lineation.

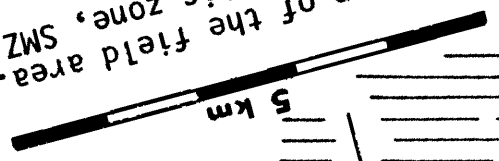
Map Units

As noted above and by earlier workers, the mylonitic zone is a stratiform, shallow-dipping zone of mylonitic rocks structurally overlying undeformed granitic rocks of the Idaho batholith. Progressively eastward, the fabric changes dramatically from dominantly isotropic rocks in the interior to strongly anisotropic rocks near the Bitterroot front. Rocks progressively acquire the characteristic mylonitic foliation and lineation encountered in the zone. As outlined on the map (Fig. 6), three units were identified, solely on the basis of fabric, for mapping purposes and petrographic study. Specific petrographic characteristics of these units will be covered in later sections.

- 1) Nonmylonitic interior - dominantly isotropic granitic rocks of the Idaho batholith; some weakly gneissic or banded.
- 2) Weakly mylonitic zone - anisotropic, weakly foliated and lineated mylonite gneiss (after Higgins, 1971), where biotite and stretched and granulated quartz and feldspar wrap around feldspar augen.

Figure 6. Generalized geologic map of the field area. Interior contacts are gradational. SMZ = strongly mylonitic zone, WMZ = weakly mylonitic zone, NMZ = nonmylonitic zone. Contacts are gradational.

- NMZ 
- WMZ 
- SMZ 



- 3) Strongly mylonitic zone - anisotropic, strongly foliated and lineated mylonite gneiss and fine grained laminated mylonite layers but containing penetrative "slickenside" striae and mica streaks on closely spaced shear surfaces.

Contacts between units are gradational over a distance of up to 150 meters. Although the degree of deformation obviously increases upward and eastward, layers, patches or rare boudins of nonmylonitic or weakly mylonitic rocks commonly are enclosed by more-deformed layers throughout the mylonitic zone. Chase (1973) and Nold (1974) report isolated mylonitic zones within nonmylonitic rocks of the interior.

Cross sections through the field area (Fig. 7) illustrate the general picture for most of the eastern flank of the Bitterroot dome. Note that the weakly mylonitic zone is thicker in section B-B' than A-A'. Lindgren's (1904) cross sections also show a general thickening of "gneissoid granite" to the south. If this portion of the dome was more mobile during offloading of the Sapphire tectonic block, conceivably the effects of mylonitization could extend to deeper tectonic levels.

Foliation

A weak foliation defined by subparallel biotite or unoriented biotite in thin bands is relatively common in otherwise isotropic rocks of the nonmylonitic interior. Penetrative planar fabric elements become more pronounced toward the Bitterroot front. In the weakly mylonitic zone, disseminated biotite, discontinuous quartz-feldspar crush layers and alignment of feldspar augen define a weak but consistent foliation and

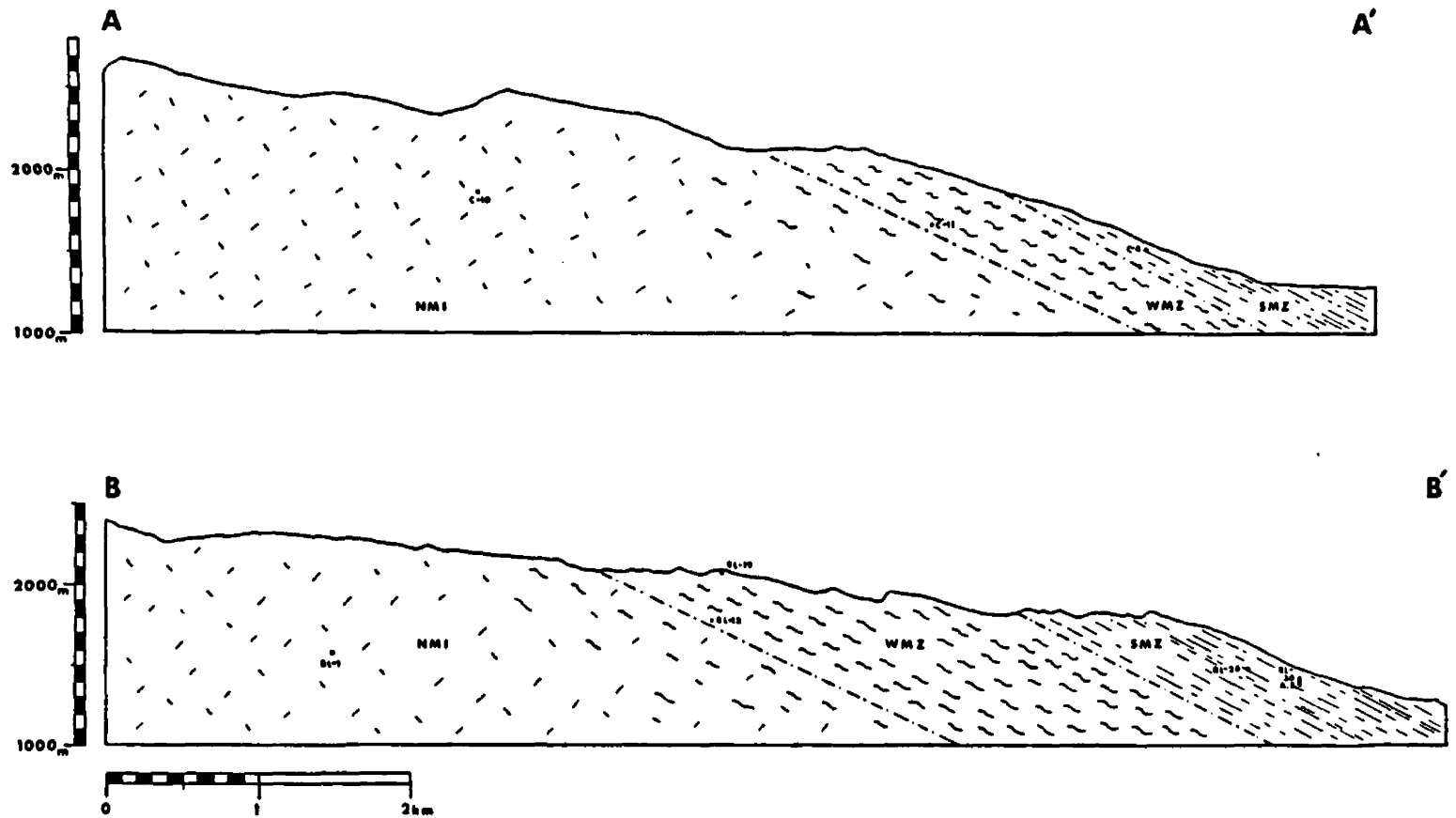


Figure 7. West-to-east cross sections through the field area with selected sample locations. NMI = nonmylonitic interior, WMZ = weakly mylonitic zone, SMZ = strongly mylonitic zone. Note that the mylonitic shear zone is thicker to the south.

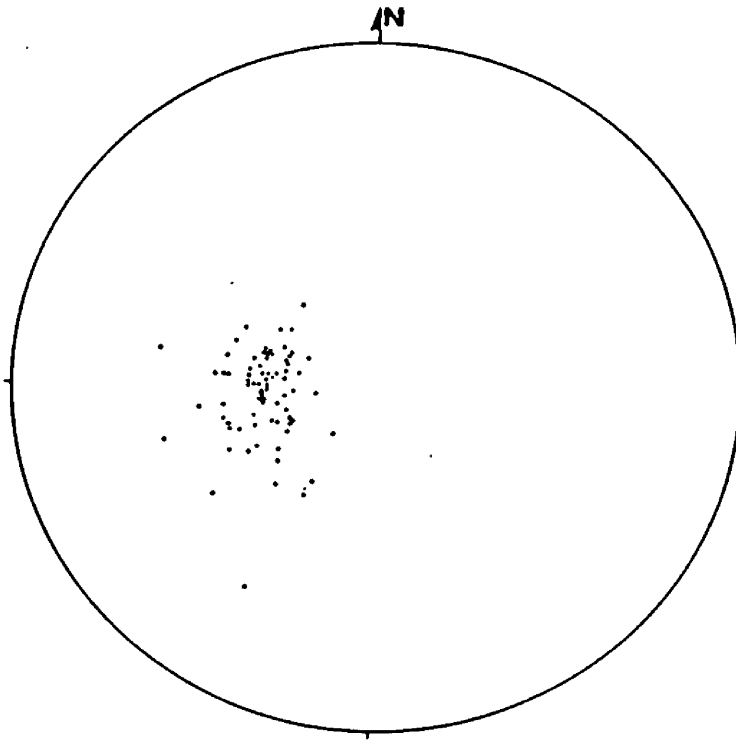


Figure 8. Orientation of poles to foliation in the mylonitic zone. 75 measurements

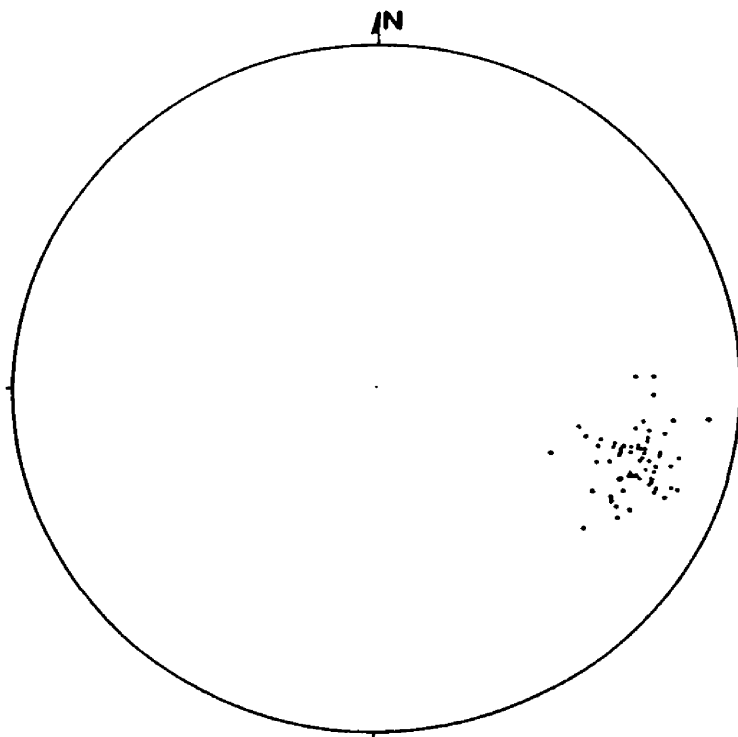


Figure 9. Orientation of mica streak and "slickenside" lineations in the mylonitic zone. 65 measurements

give the rock a uniform gneissic appearance. Further development of the crush layers and segregation of quartz, potassium feldspar and imbricated augen into distinct layers and rods imparts a strong foliation on strongly mylonitic rocks. In addition, the strongly mylonitic zone is penetrated by parallel discrete slip surfaces containing "slickenside" striae exposed on foliation joint planes. A plot of poles to foliation (Fig. 8) show little variation in the mylonitic units.

Lineation

Alignment of the long axis of feldspar augen and quartz rods within the foliation in addition to mica streaks and "slickenside" striae on shear surfaces, define a strong set of uniform parallel lineations plunging eastward down dip. Figure 9 shows the uniformity of the mica streak and "slickenside" lineation which on average trend 106° and plunge 24° . Figure 10 is a sketch of a typical sample from the strongly mylonitic zone which exhibits these features. As noted by Hyndman (1980), this penetrative slickenside lineation lying within a mylonitic foliation maintains a nearly constant orientation across the whole Bitterroot dome, is strongest in the east within the mylonitic zone and gradually flattens westward across the dome.

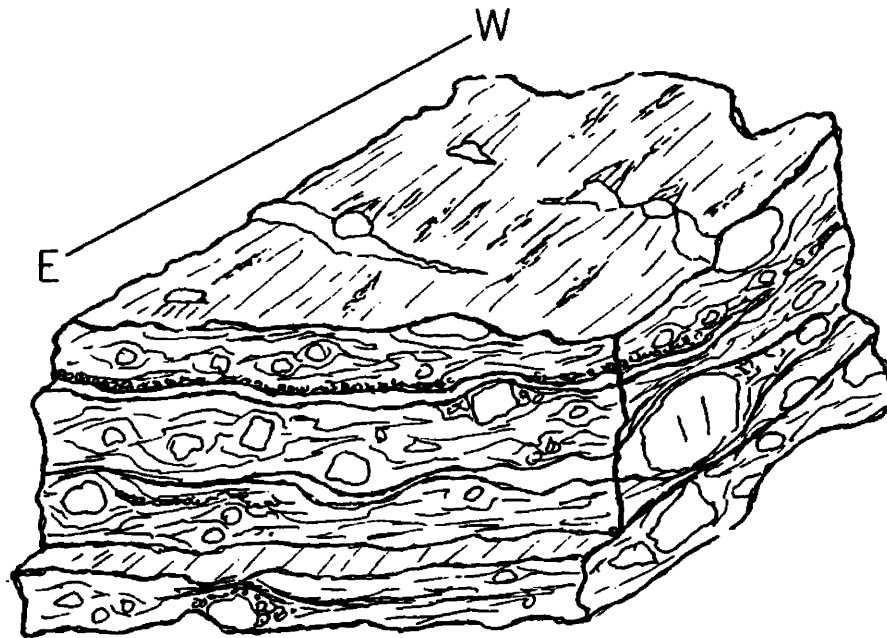


Figure 10. Sketch of typical strongly mylonitic mylonite gneiss sample showing mesoscopic features; foliation (layering and shear surfaces), lineation (mica streaks and "slickensides"), and augen orientation and shape. The largest augen in this sample (GS-4) is about 4 cm long.

CHAPTER IV

DESCRIPTIVE PETROGRAPHY

General Statement

For mapping, structural, and petrographic work the area was conveniently divided into three zones (following Chase, 1973 and Clark, 1979) in which at least six distinctly different rock types occur. Distinction between the three zones is textural and transition from one zone to the next is gradational over a distance of about 150 meters. Except for local zones of high strain or thin concordant mafic dikes, sharp contacts do not exist. Although the mesoscopic and microscopic fabric changes dramatically from nonmylonitic rocks of the interior to strongly sheared mylonites at the Bitterroot front, the mineralogy and chemistry (of similar rocks mapped by Chase, 1973) show little variation.

Nonmylonitic Interior

Nonmylonitic rocks of the eastern part of the Bitterroot lobe of the Idaho batholith vary in composition and structure from foliated quartz diorite to massive megacryst-bearing granite (Chase, 1976). The majority of rocks in this study are granite (see Streckeisen, 1973) or granodiorite but range to tonalite (see Fig. 11). Average modes and modal ranges are shown in Table 1; individual analyses can be found in Appendix 1. Lindgren (1904), Langton (1935), Ross (1950), Chase (1973), and Clark (1979) report similar modes for the batholith. Irregular

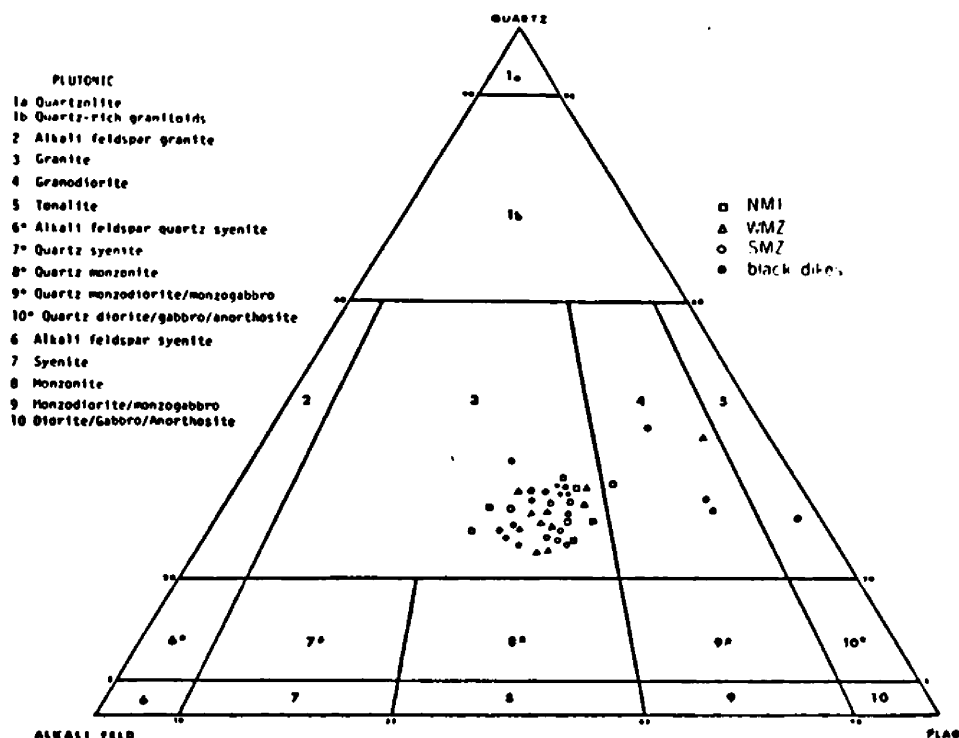


Figure 11. Plot of modes of thin section samples from non-mylonitic and mylonitic units on IUGS classification of igneous rocks.

Table 1. Average modes (modal ranges) of nonmylonitic and mylonitic samples

Unit	Nonmylonitic interior	Weakly mylonitic zone	Strongly mylonitic zone
Mineral	(9 analyses)	(11 analyses)	(20 analyses)
Plagioclase	38 (28-41)	34 (27-50)	35 (25-55)
Potassium feldspar	27 (20-35)	28 (5-35)	28 (10-39)
Quartz	27 (21-32)	26 (20-38)	26 (20-30)
Biotite	5 (4-7)	5 (3-6)	4 (1-7)
Muscovite	2 (1-5)	2 (tr-3)	2 (0-10)
Plagioclase			
Chlorite	tr-1	tr-2	tr-4
Opaque minerals	tr	tr	tr
Apatite	tr	tr	tr
Zircon	tr	tr	tr
Sericite	tr	tr	tr
Rutile	tr	tr	tr
Sphene	tr	tr	tr
Sillimanite	tr	tr	

pegmatite veins, biotitic schlieren, and biotitic xenoliths are widely distributed throughout the batholith and may be found in the mylonitic zone as well.

Light gray, equigranular, medium to coarse-grained, allotriomorphic- to hypidiomorphic-granular texture and isotropic fabric dominate. However, some areas are porphyritic containing poorly- to well-developed potassium feldspar megacrysts or are weakly foliated, defined by sub-parallel disseminated biotite or thin biotite-rich bands giving the rock a slightly gneissic appearance. In thin section, particularly in samples closer to the overlying weakly mylonitic zone, small non-penetrative patches of crushed rock are interstitial to larger grains. Plates 1 and 2 show typical textural characteristics found in the non-mylonitic interior.

Medium to coarse-grained, subhedral and anhedral plagioclase (oligoclase-andesine) grains commonly contain albite, Carlsbad, albite-Carlsbad and albite-pericline twins. Some grains are weakly zoned with normal, reverse, and oscillatory zoning. Plagioclase is commonly weakly sericitized along twins or cracks and contains inclusions of quartz, biotite or smaller plagioclase crystals. Small euhedral - subhedral grains often occur as twinned inclusions (sometimes rimmed by albite) in large potassium feldspar megacrysts. Small irregularly shaped myrmekitic plagioclase commonly borders plagioclase in contact with potassium feldspar and appears in the nonpenetrative patches of crushed rock between grains. Plagioclase rarely exhibits any preferred orientation, strain shadows, or bent twin lamellae.

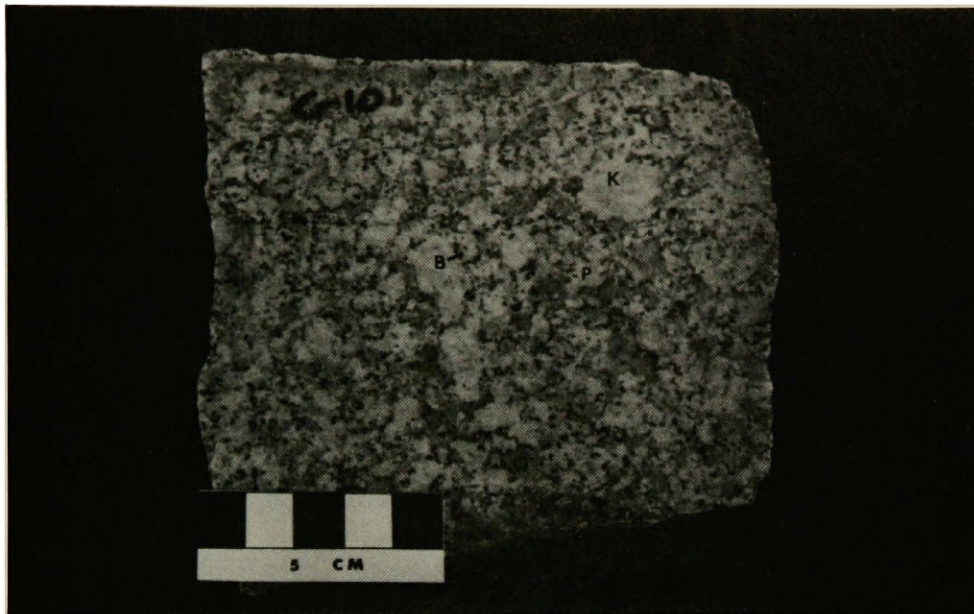


Plate 1. Mesoscopic fabric of nonmylonitic interior granite-granodiorite sample C-10. Note hypidiomorphic-granular, isotropic fabric with poorly developed K-feldspar megacrysts and randomly oriented biotite. B = Biotite, K = K-feldspar, P = Plagioclase, Q = Quartz.

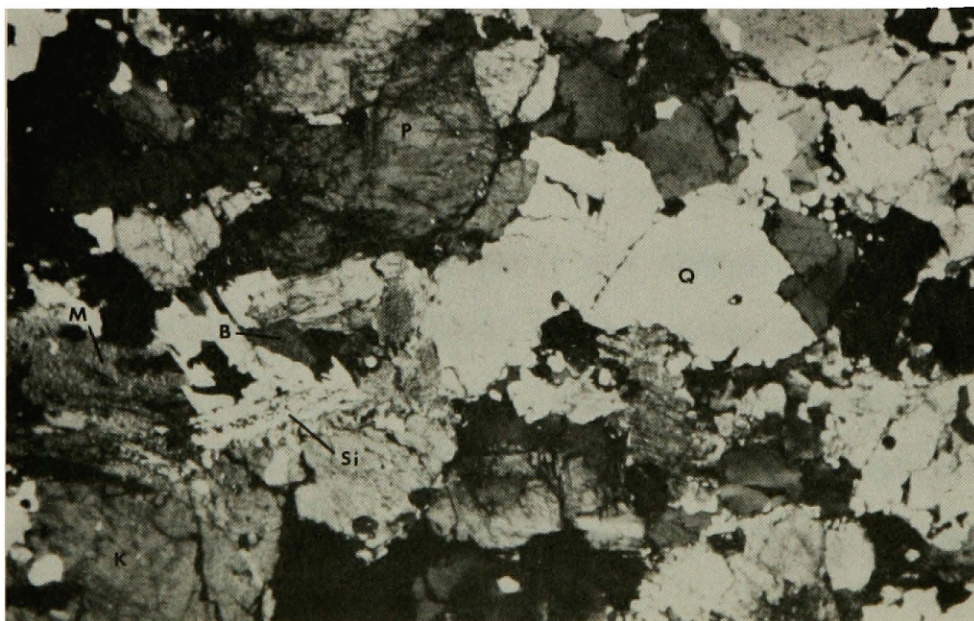


Plate 2. Photomicrograph of nonmylonitic sample BL-3. Field of view is 8.2 mm. Quartz shows strain shadows and K-feldspar is weakly strained. Note that no preferred orientation of grains is apparent in this sample. Sillimanite (Si) occurs in muscovite (M).

Anhedral to subhedral potassium feldspar (orthoclase or microcline) occurs as medium-sized grains and as large megacrysts. Carlsbad twins occur in many grains and patches of faint microcline grid twins appear in slightly undulose grains and megacrysts. Commonly, the megacrysts are poikilitic with crystallographically-oriented inclusions of plagioclase, biotite, and quartz. Some megacrysts are perthitic containing thin, wavy bead- and string-type exsolutions or consist of poorly developed patches and engulf virtually every other mineral. Although no preferred orientation was observed, potassium feldspar near the overlying weakly mylonitic zone, shows weak undulatory extinction.

Interstitial, anhedral quartz is always undulose, medium- to fine-grained with sutured or embayed grain boundaries, or contains polygonal subgrains. Quartz is a common inclusion in feldspar, and larger patches and grains contain rare planar bubble trains.

Fine biotite flakes, commonly partially or completely altered to chlorite occur along grain boundaries or as inclusions in feldspar. Biotite appears unoriented in homogeneous and banded rocks in the interior and weakly oriented in gneissic zones. Bands are biotite-rich but individual grains show no mesoscopic preferred orientation. Zircon occurs in biotite and chloritic biotite commonly contains fine rutile needles, sphene or opaque minerals. Apatite occurs with biotite or interstitially.

Muscovite occurs as thin stringers along grain boundaries or as larger grains replacing feldspar. It is commonly bent and several samples contain sillimanite (e.g. BL-4, 5 & RL-3, 8, 10). Garnets occur in one thin section and were observed in several outcrops.

Weakly Mylonitic Zone

As shown in Table 1, the mineralogy and composition of this structural unit is virtually identical to rocks of the nonmylonitic interior. Even fine textural details and mineral associations remain the same. In the field area this zone ranges from about 500 to 700 meters thick. The distinction between this zone and the underlying nonmylonitic interior lies solely in a change in the mesoscopic and microscopic fabric from dominantly isotropic to anisotropic in nature. Feldspars are dimensionally oriented down-dip in a weak foliation defined by thin quartz-feldspar crush layers and subparallel micas which wrap around feldspar augen or uncrushed rock fragments. The rock in this zone is a mylonite gneiss (after Higgins, 1971) and the foliation becomes more pronounced upward through the unit everywhere maintaining a uniform eastward dip. Foliation shear surfaces in the upper part of the zone contain a mica-streak lineation.

Plagioclase forms lensoid or round augen commonly with rough edges, weak stain shadows and thin discontinuous twin lamellae probably formed by deformation. These lamellae often pinch out or are kinked and displaced slightly. Plagioclase also occurs as small rounded grains in crush layers or lenses with potassium feldspar and quartz, and as inclusions in potassium feldspar megacrysts. Myrmekite is in many cases the dominant plagioclase in crush layers and occurs as undeformed grains embaying (replacing?) potassium feldspar megacrysts, patches, and layers.

Potassium feldspar occurs as megacrysts as in the nonmylonitic interior and as lensoid augen, small rounded grains in crush layers and lenses, and in discontinuous layers leading from pressure shadows of

both feldspars. In general, potassium feldspar in this zone is more deformed evidenced by more undulatory patchy extinction. Also, faint microcline grid twins occur in the more deformed grains.

Quartz occurs as undulose interstitial grains, as inclusions in feldspar, in the crush layers and as composite lenses and discontinuous layers parallel to foliation. Some grains contain the bubble trains mentioned above and very faint evenly spaced deformation lamellae in grains near extinction.

Disseminated biotite and muscovite wrap around closely packed feldspar augen and define the weak foliation. Biotite is generally partially altered to chlorite or muscovite and contains the accessory minerals mentioned. Sillimanite occurs in one sample from this zone.

Plates 3, 4, and 5 show characteristic textures encountered in this zone.

Strongly Mylonitic Zone

The strongly mylonitic zone, the highest structural unit, is up to 520 meters thick and forms the uniform east-dipping front of the Bitterroot Range. It has been described and called "gneiss" (Lindgren, 1904), older gneiss (Langton, 1935), border-zone gneiss (Ross, 1950), and frontal zone gneiss by most recent workers including Anderson (1959), Berg (1968), Chase (1961), Groff (1954), and Wehrenberg (1972). Again, the mineralogy, composition (see Table 1) and textural details remain similar to nonmylonitic and especially weakly mylonitic rocks underlying this zone. However, the anisotropic character, both mesoscopically and microscopically, of rocks in this zone is more pronounced

and a strong foliation results from: continuous crush layers containing equigranular feldspar, quartz and mica; subparallel biotite; layers or rods of clean segmented quartz; layers of potassium feldspar; and thin closely spaced shear surfaces containing the characteristic mica streak and "slickenside" lineation encountered in this zone. The lineated shear surfaces, and general finer grain size resulting from a higher percent crushed matrix along with a more laminated aspect distinguish this zone from the underlying, less mylonitized zones. Rocks in this zone are mylonite gneisses and "blastomylonites" after Higgins (1971). See plates 6, 7, and 8.

Aligned feldspar augen commonly define a weak lineation pointing down-dip in the foliation, locally are imbricated or form augen rich layers. Augen appear suspended in a ductile matrix which flows around them. Associated pressure shadows are characteristically filled with potassium feldspar, but also quartz, mica, crushed matrix or chips plucked from the individual augen. The thin lineated shear surfaces generally follow earlier crush layers but also cut and displace augen (see Plate 9). Other common textures affecting augen such as plucked-boundary, goatee, granular and shear-step or pull-apart are shown in Plates 10 and 11.

Rounded plagioclase augen commonly contain thin (deformation?) twins which pinch out, change extinction across strain shadows (see plate 12), are kinked, bent or broken-up and annealed. Plagioclase also occurs as small rounded grains in crush layers. Much of this is myrmekitic and myrmekite commonly embays potassium feldspar megacrysts

or augen, layers and pressure shadows. Some myrmekite is twinned.

Potassium feldspar exhibits textures similar to plagioclase but augen commonly are lens-shaped or nearly euhedral and grade into potassium-feldspar-rich segmented layers. Few augen are perthitic but many exhibit patchy undulatory extinction and faint isolated grid-twins. Some are randomly oriented and appear to cut crush zones. Larger megacrysts are poikilitic and contain oriented plagioclase, quartz, or biotite or strongly deformed annealed plagioclase as in Plate 13. Potassium feldspar also occurs as small rounded grains in the crush layers.

Quartz occurs as fine equant grains in crush layers and pressure shadows and as flattened elongate grains in layers and rods. Planar bubble trains or faint deformation lamellae appear in but a few grains.

Subparallel biotite, commonly altered to chlorite and/or muscovite, and muscovite occur individually or as thin stringers within crush zones or along shear surfaces. Muscovite commonly bends around augen and is undulose or is recrystallized into polygonal arches.

Apatite, sphene, zircon, rutile, and opaque accessory minerals appear in biotite or chlorite. Apatite, sphene and garnet also occur in crush layers.

Black mylonite. Commonly within the strongly mylonitic zone and locally within lower units, black fine grained "streaked out" looking mylonite layers from about 1 to 30 centimeters thick parallel or cut the enclosing augen gneiss at slight angles. These fine-grained laminated

mylonitic layers, herein called black mylonite, commonly display sharp contacts with no intermediate zone, are generally tabular or pinch and swell over tens of meters. In thin section, they resemble a finer-grained version of strongly mylonitic rock. They rarely possess the lineated shear surfaces normally found in the strongly mylonitic zone except on the contact with coarser augen gneiss. Where they cut the enclosing gneiss, it is commonly at angles of less than 5 degrees and at a shallower dip.

Uniformly layered and nearly equigranular varieties exist. The layered or laminated black mylonite contains continuous nearly monomineralic laminations of segmented quartz, potassium feldspar and quartz-feldspar crush zones. Biotite and/or muscovite are disseminated and oriented or occur as thin continuous stringers. Feldspar augen where present, are tiny and round plagioclase, or lense-shaped potassium feldspar, and grade laterally into layers. Augen characteristically contain deformation twins or a patchwork of disjointed subgrains and appear as though they are beginning to break up into smaller grains (see Plate 14). Plagioclase commonly is pulled apart, and virtually all grains are deformed except perhaps myrmekite replacing potassium feldspar. The equigranular variety contains broken and separated sparse augen is essentially a crush-zone matrix.

In Canyon Creek and elsewhere, nearly euhedral potassium feldspar megacrysts are unoriented or weakly oriented, and appear to cut the strongly sheared matrix. Unfortunately no thin sections include such megacrysts but obviously they formed late or after shearing in the zone.



Plate 3. Typical outcrop of weakly mylonitic zone mylonite gneiss near the top of the zone north of Camas Lake. Note the alignment of feldspar augen within the foliation, but foliation joints and lineated shear surfaces are absent.

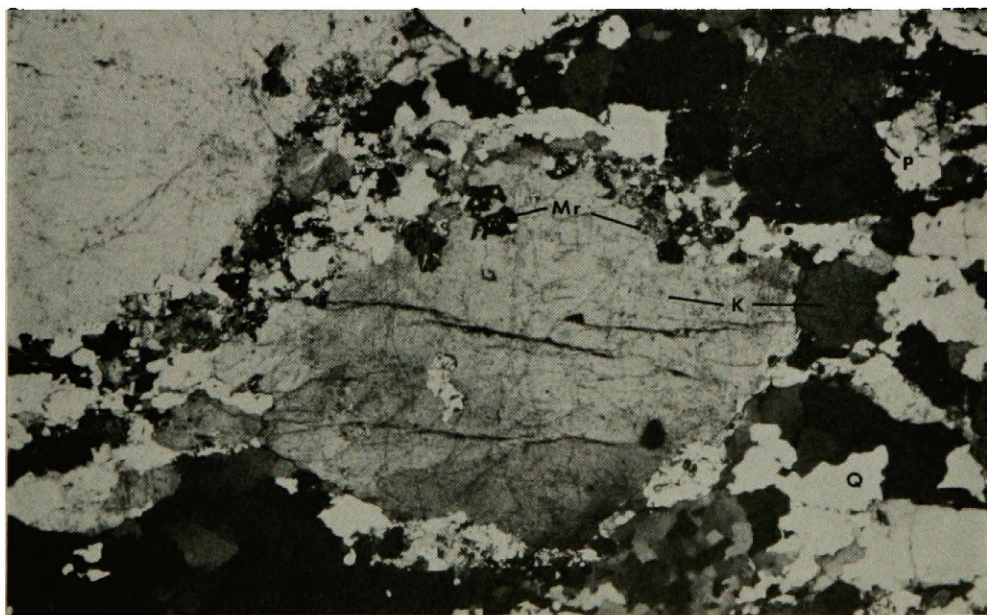


Plate 4. Photomicrograph of weakly mylonitic sample RL-13a. Field of view is 8.2 mm. Discontinuous crush layers, quartz layers and subparallel biotite wrap around feldspar augen. Thin deformation(?) twins appear in plagioclase. K-feldspar occurs as augen and in pressure shadows. Myrmekite (Mr) is common in crush zones adjacent to and replacing K-feldspar.

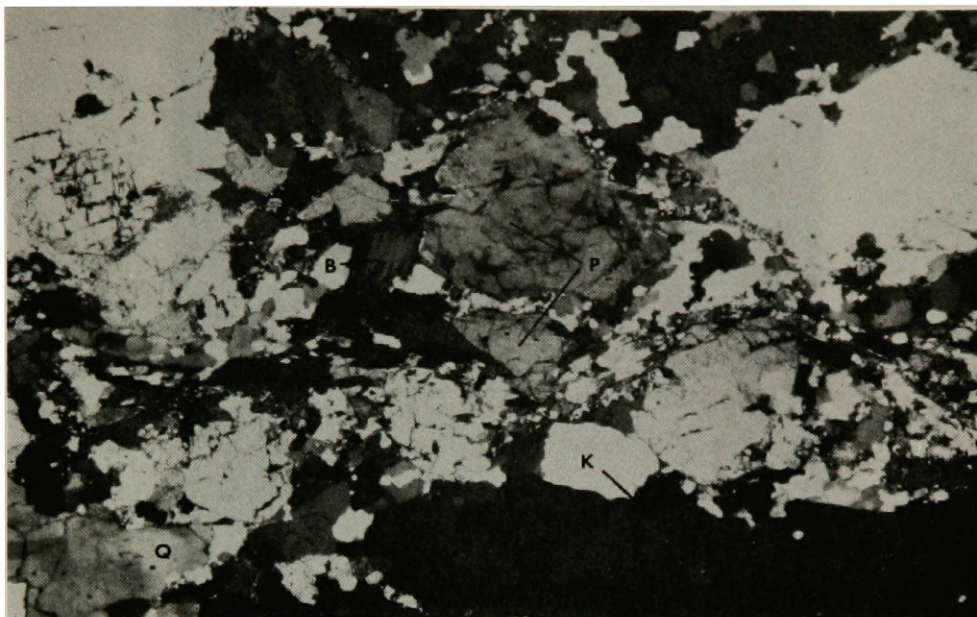


Plate 5. Photomicrograph of weakly mylonitic sample RL-13. Field of view is 8.2 mm. Thin crush layers and quartz layers are discontinuous. Note the broken grain of plagioclase in the center and the large subhedral K-feldspar megacryst (extinct) which appears to be replacing the matrix.



Plate 6. Photo looking north at an outcrop of strongly mylonitic zone mylonite gneiss (top) and black mylonite near the mouth of Roaring Lion Creek. The lighter is 8 cm long and is lying on a slickensided shear surface. Foliation in the black mylonite dips at a slightly shallower angle than the enclosing gneiss.

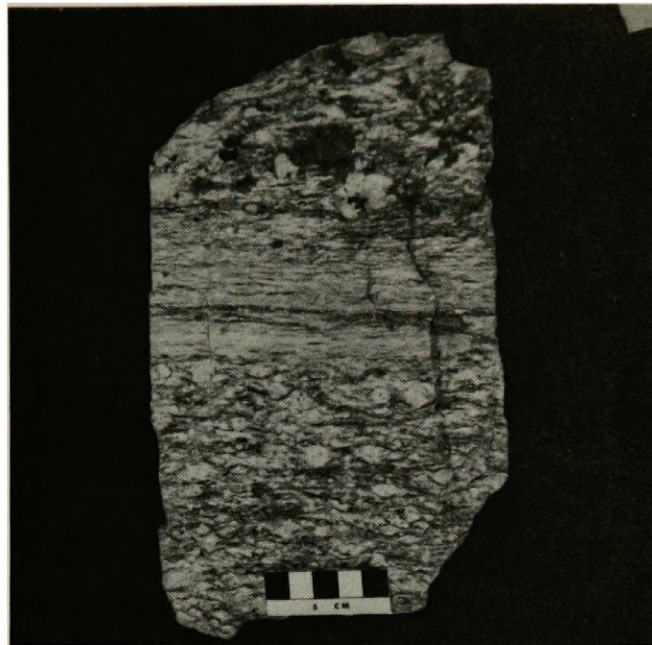


Plate 7. Sample from the strongly mylonitic zone of typical mylonite gneiss and white, fine-grained, streaked-out white mylonite layer. These white mylonites are zones of high strain and appear to be sheared pegmetites.

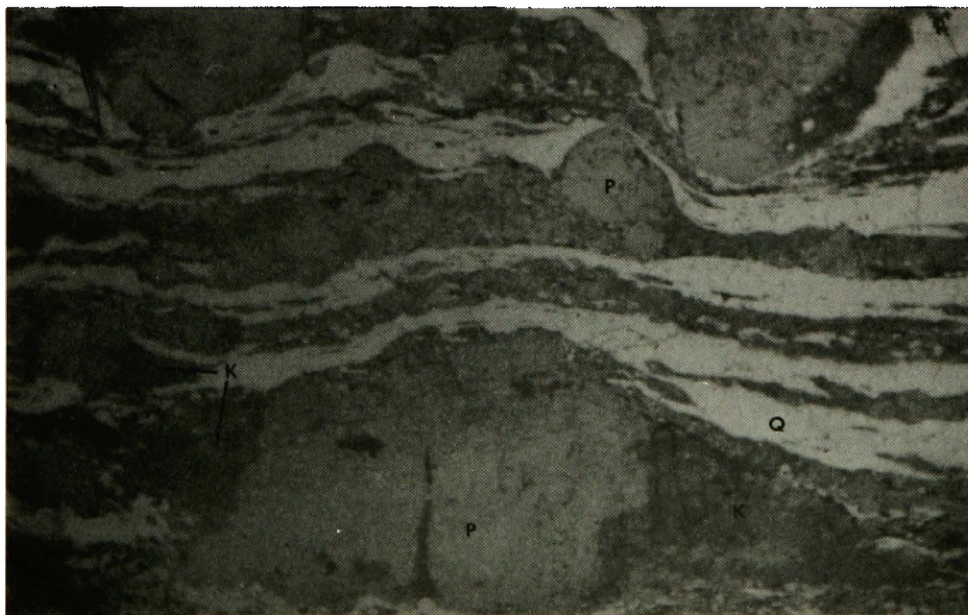


Plate 8. Photomicrograph of strongly mylonitic sample RL-29a in plain light. Field of view is 8.2 mm. Note continuous quartz layers, crush layers and rounded plagioclase augen with K-feldspar in pressure shadows.

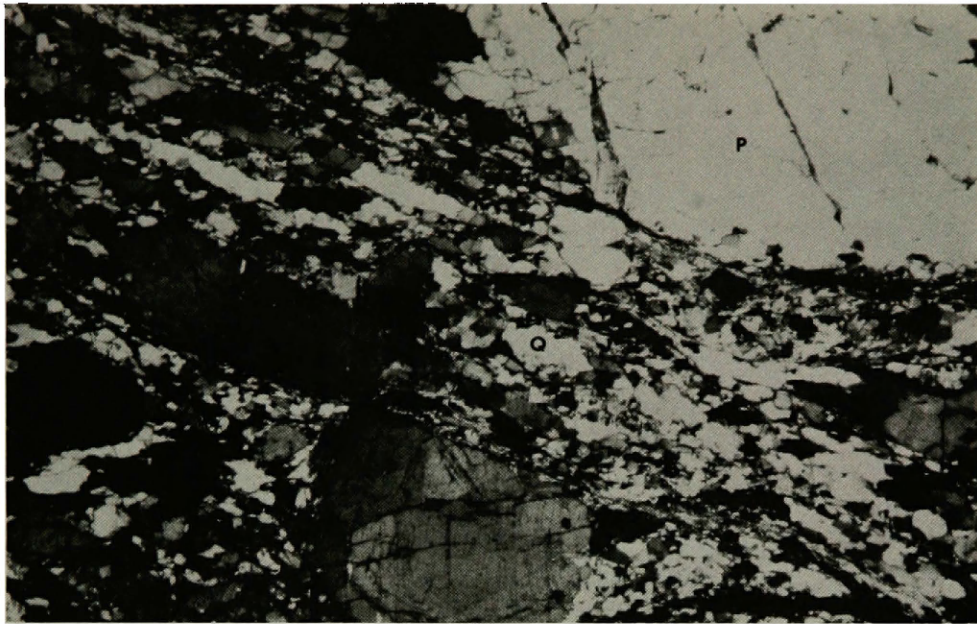


Plate 9. Photomicrograph of strongly mylonitic sample C-4a. Field of view is 8.2 mm. Thin muscovite rich shear surfaces parallel the quartz-rich crush layer matrix and offset a plagioclase grain. Note the tension fractures in the plagioclase augen at the top of the photo.

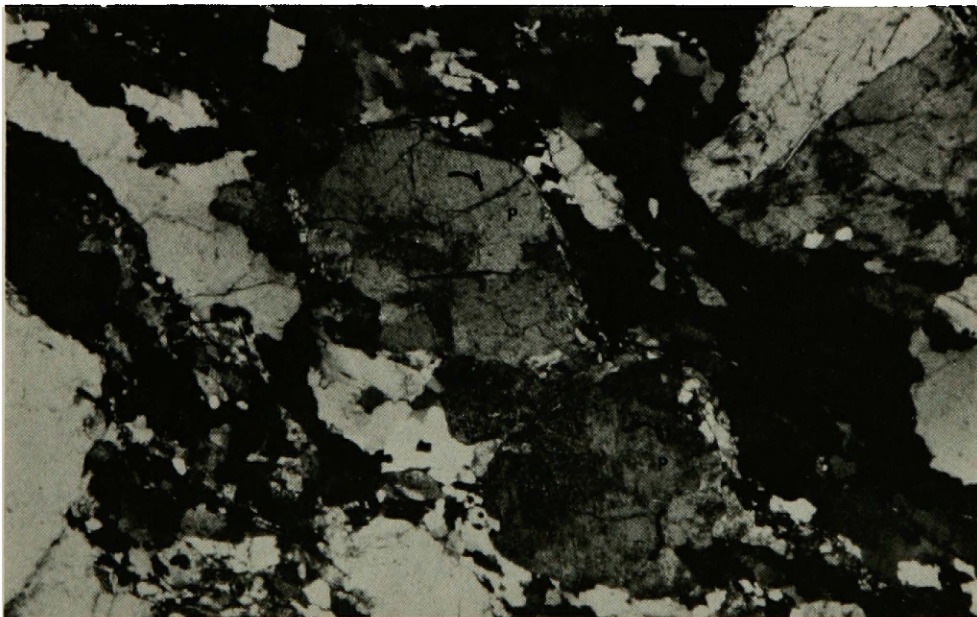


Plate 10. Photomicrograph of strongly mylonitic sample RL-25a. Field of view is 8.2 mm. The plagioclase augen has been fractured and rotated displaying shear-step texture. Arrows show sense of rotation.

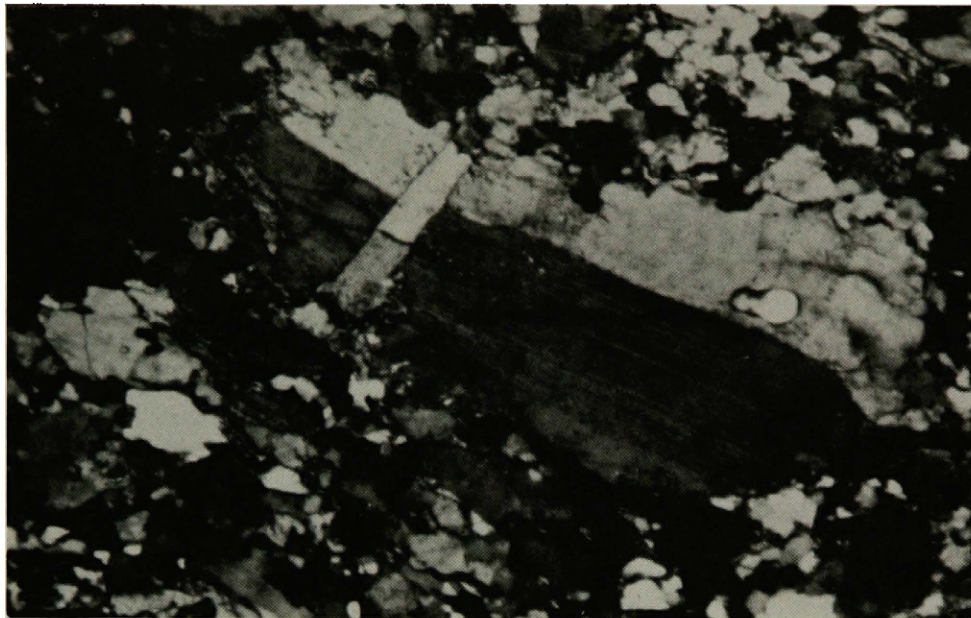


Plate 11. Photomicrograph of strongly mylonitic sample GS-1a. Field of view is 2 mm. Quartz fills a fracture in a pulled apart plagioclase grain.

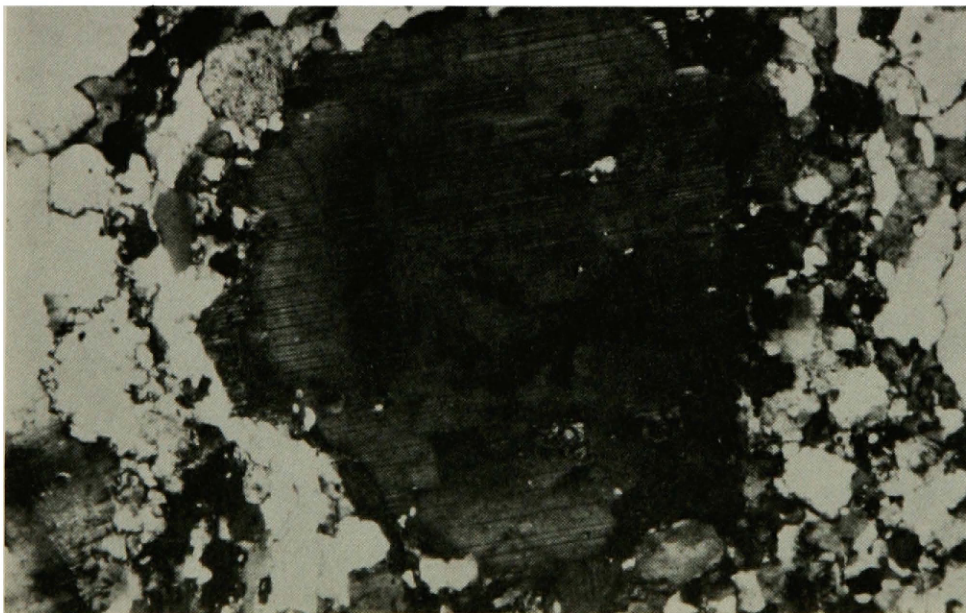


Plate 12. Photomicrograph of strongly mylonitic sample RL-30b. Field of view is 2 mm. Deformation (?) twins change extinction across strain shadows in plagioclase. Faint microcline grid twins appear in a strained K-feldspar grain (lower left corner).

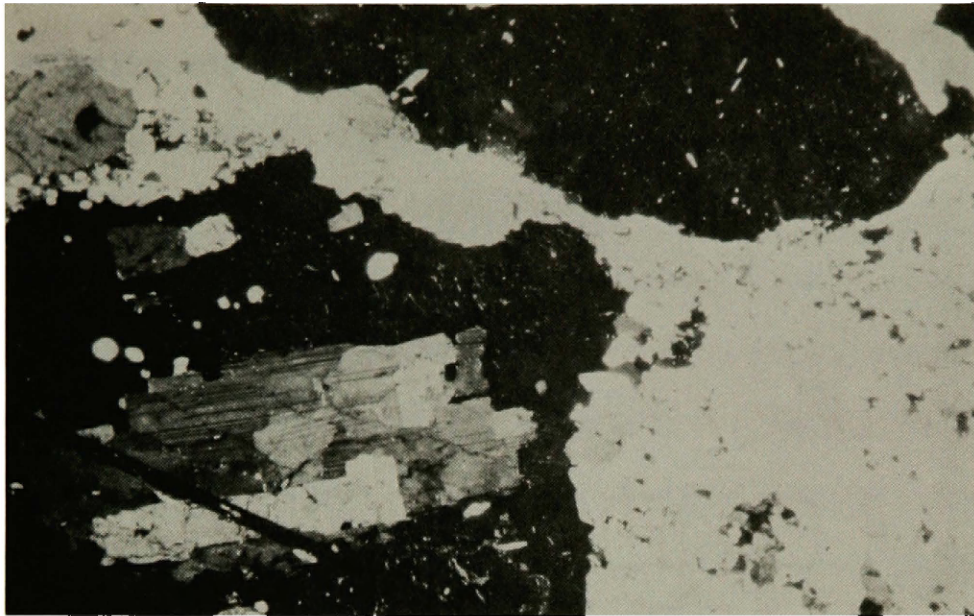


Plate 13. Photomicrograph of strongly mylonitic sample C-4b. Field of view is 8.2 mm. Nearly euhedral, broken and annealed plagioclase is enclosed in a relatively undeformed K-feldspar megacryst (extinct). This inclusion and smaller ones appear to be crystallographically oriented.

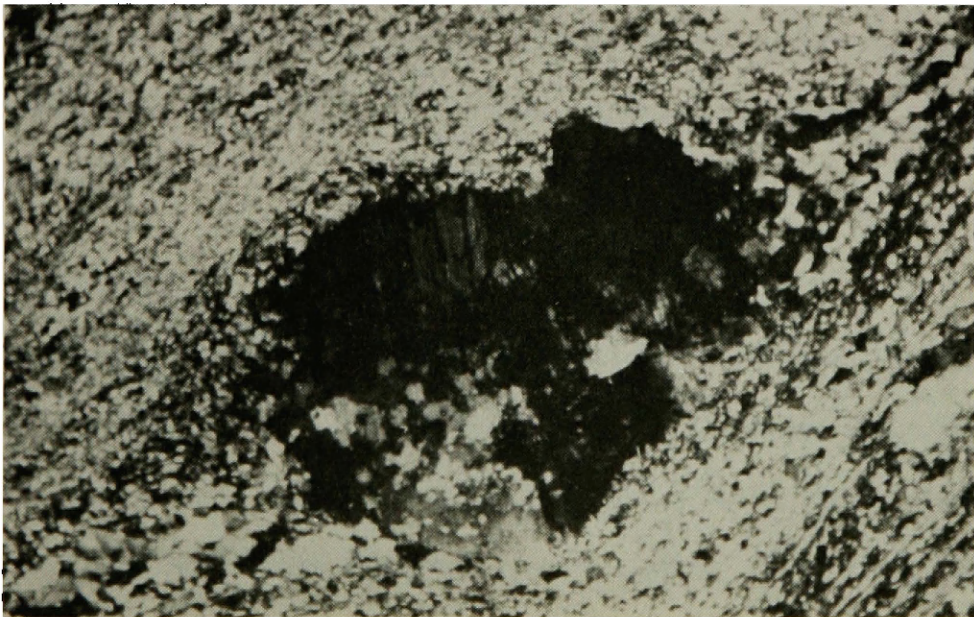


Plate 14. Photomicrograph of strongly mylonitic black mylonite sample C-9a. Field of view is 8.2 mm. Rounded, crushed, plagioclase augen is beginning to break up into smaller grains and become part of the black mylonite matrix.

Black mylonite and white mylonite layers described below suggest that intense local shearing occurred in these zones.

White mylonite. Thin white streaked-out layers, or augen- plus quartz-rich layers in the mylonitic zone appear to be sheared pegmatites. Texturally, they commonly resemble the black mylonite but contain little biotite, and in samples from this area little or no muscovite and more apatite than usual which occurs in and cuts plagioclase-rich crush zones.

Black dikes. Near the Bitterroot front, in Roaring Lion Creek, a sequence of concordant fine-grained black dikes are interlayered with white mylonite and normal mylonite gneiss. Compositionally they are tonalite with no potassium feldspar or muscovite. Although these were not studied in detail, they are deformed and weakly foliated as defined by subparallel biotite. In a sample collected by Don Hyndman at the mouth of Sweathouse Creek, they appear to possess a weak crenulation cleavage. Lindgren (1904) noted a similar sequence near the mouth of Sawtooth Creek Canyon.

Chemical Similarities

The near identical mineralogy, modes and modal ranges of non-mylonitic and mylonitic zones evident in Table 1 plus the microscopic and mesoscopic structural characteristics leave little doubt that rocks in this part of the dome were derived from a common protolith, granitic rocks of the Idaho batholith.

Likewise, Chase's (1973, pp. 8 and 9) whole-rock chemical analyses and variation diagram from similar rocks and zones he mapped farther

north show no deviation from a normal chemical variation and support this conclusion. Appendix 2 includes Chase's analyses and variation diagram.

CHAPTER V

DESCRIPTIVE MICROSCOPIC STRUCTURAL ANALYSIS

General Statement

Orientation diagrams for Quartz [0001] (Figs. 12-20) and biotite {001} (Figs. 22-24) were prepared to statistically analyze and compare the fabric symmetry of nonmylonitic interior rocks with those in the mylonitic zone. Standard petrofabric methods outlined by Turner and Weiss (1963, pp. 194-225) were employed and diagrams were rotated (where necessary) and oriented relative to the mesoscopic foliation and lineation, or to geographic coordinates in nonmylonitic rocks. Diagrams were contoured using the grid method first and refined using the free-counter method (see Turner and Weiss, 1963, pp. 61-62). Contour intervals generally are consistent throughout.

The location of each of the following samples is plotted on the cross-sections (Fig. 7).

Nonmylonitic interior:

RL-1b, granodiorite

C-106, granodiorite

Weakly mylonitic zone:

RL-13b, granite (mylonite gneiss)

RL-19b, granite (mylonite gneiss)

C-11b, granodiorite (weakly foliated mylonite gneiss)

Strongly mylonitic zone:

RL-A, granite (mylonite gneiss)

RL-B, granite (mylonite gneiss)

C-4b, granite (mylonite gneiss)

RL-26b, granite ("black mylonite")

RL-30b, granite pegmatite(?) ("white mylonite")

Fabric axes were selected as follows

RL-1b and C-10b, \underline{X} = geographic east-west

\underline{Y} = geographic north-south

\underline{Z} = vertical (normal to XY plane)

C-11b \underline{X} = parallel to foliation dip (25° E)

\underline{Y} = geographic north-south (approx. foliation strike)

\underline{Z} = normal to XY plane of foliation

RL-13b, 19b, \underline{X} = parallel to lineation

26b, 30b, RL-A
RL-B and C-4b \underline{Y} = normal to lineation in foliation

\underline{Z} = normal to XY plane of foliation

Quartz C-axis Orientation

In samples collected from the nonmylonitic interior (Fig. 12 and 13), quartz axes [0001] show nearly random orientation. However, maxima outlined in Figure 12 (C-10b) and a weak but general concentration of points in Figure 13 (RL-1b) may define a great circle girdle or plane oriented vertically trending about 30° (geographically N30°E). The statistical significance of this possibility is difficult to evaluate considering the number of C-axes measured, the lack of mesoscopic foliation and

lineation, and the wider spread of points in these diagrams compared to following diagrams.

Weakly mylonitic samples (Figs. 14, 15 and 16) display great circle girdle patterns with associated double or single maxima. The girdle axes lie close to X (lineation) and maxima are arranged almost symmetrically about the XY plane (foliation). Strongly mylonitic samples (Figs. 17, 18, 19 and 20) show patterns and relationships similar to the weakly mylonitic diagrams with respect to fabric axes and planes.

The fact that girdles and their axes and associated single or double maxima do not precisely coincide or are not perfectly symmetric about the selected fabric axes is not disturbing. The probable source of error lies with measuring the orientation of fabric axes and planes from the mesoscopic hand specimen or outcrop from which the thin section was cut and oriented. The number of grains measured also influences location of maxima and contours. As Turner and Weiss (1963, p. 431) note "...neither hypothetical orientation mechanisms nor detail of quartz-axis patterns can enter into our interpretation of preferred orientation of quartz in tectonites. Strength and position of individual maxima in relation to schistosity and lineation are taken into account only to the extent that they define the symmetry of the quartz subfabric and of the tectonite fabric as a whole. The significant property of a quartz pattern is its symmetry." In this light, the symmetry of the quartz C-axis subfabric for rocks in the mylonitic zone (both weakly and strongly mylonitic) is orthorhombic. The planes defined by the fabric axes X, Y, Z, roughly

coincide with the three mutually perpendicular planes of orthorhombic symmetry. The symmetry of the quartz axis fabric for nonmylonitic rocks is more problematic. If needed the pattern is statistically random, then the symmetry is spherical rendering the rocks nearly isotropic with respect to quartz C-axis orientation. However, if the hint of a girdle pattern exists, then their symmetry would be orthorhombic.

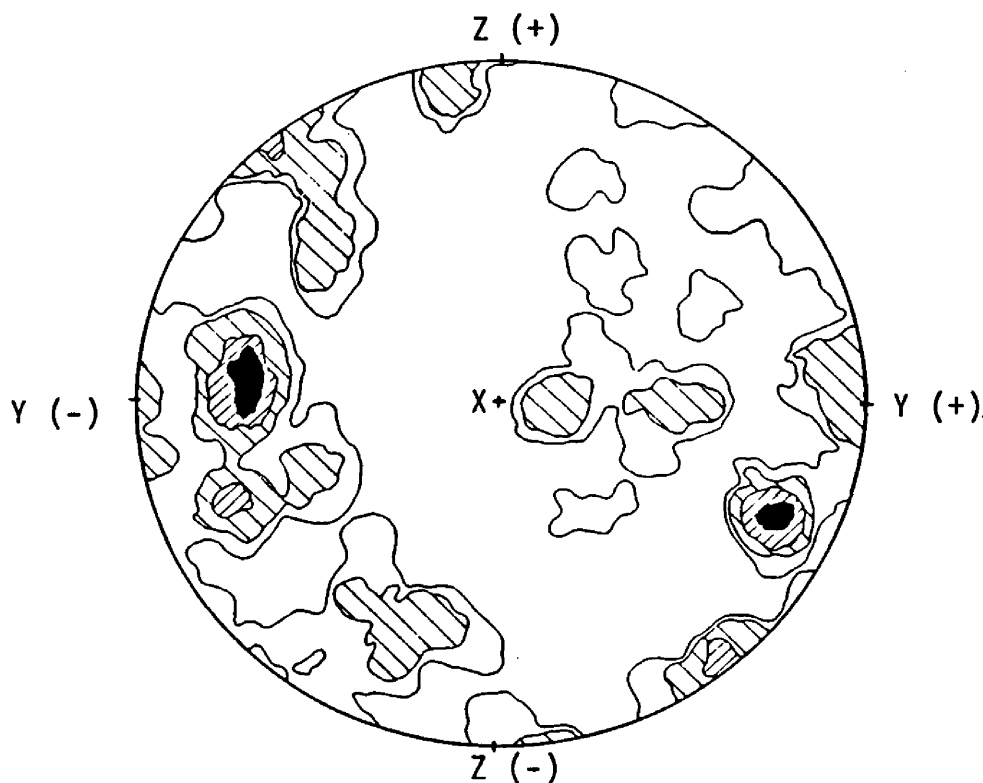


Figure 12. Orientation diagram for nonmylonitic sample C-10b; 201 quartz [0001]. Contours are 6, 4, 2, and 1%.

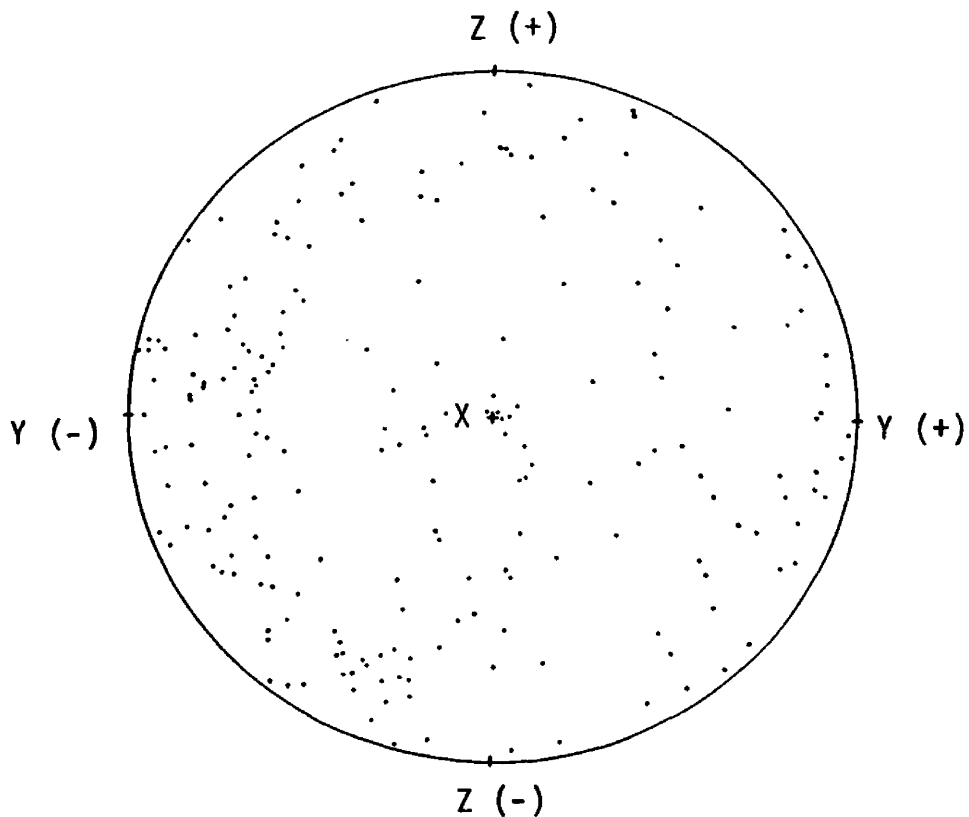


Figure 13. Orientation diagram for nonmylonitic sample RL-1b; 207 quartz [0001].

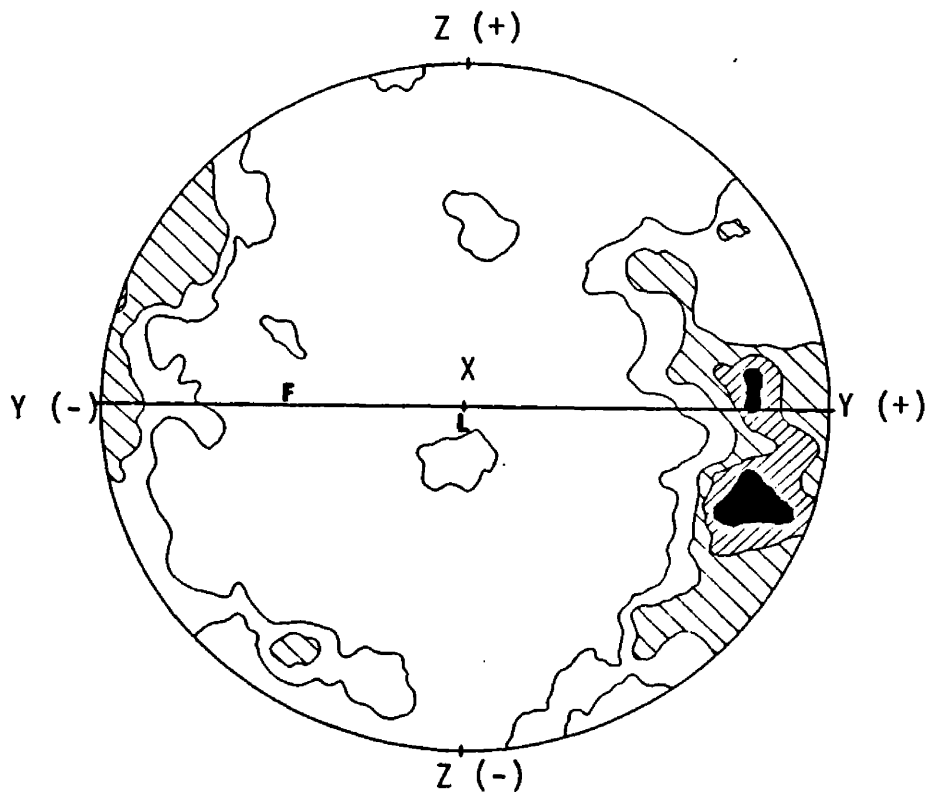


Figure 14. Orientation diagram for weakly mylonitic sample C-11b; 290 quartz [0001]. Contours are 6, 4, 2 and 1%. F - foliation, L = lineation.

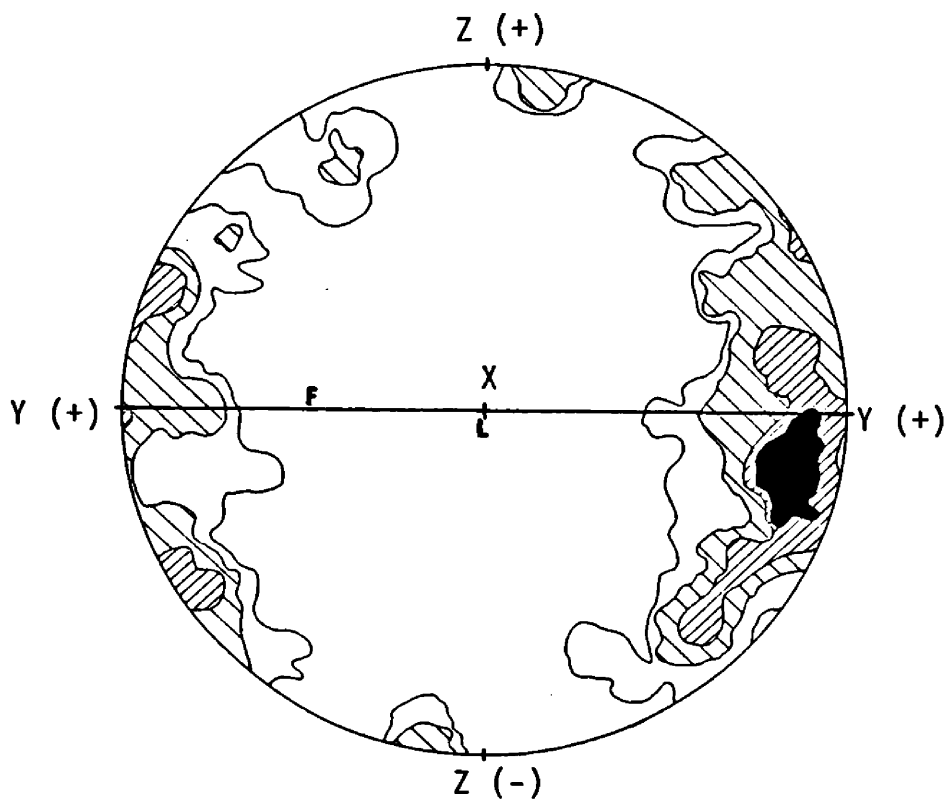


Figure 15. Orientation diagram for weakly mylonitic sample RL-13b; 206 quartz [0001]. Contours are 6, 4, 2 and 1%.

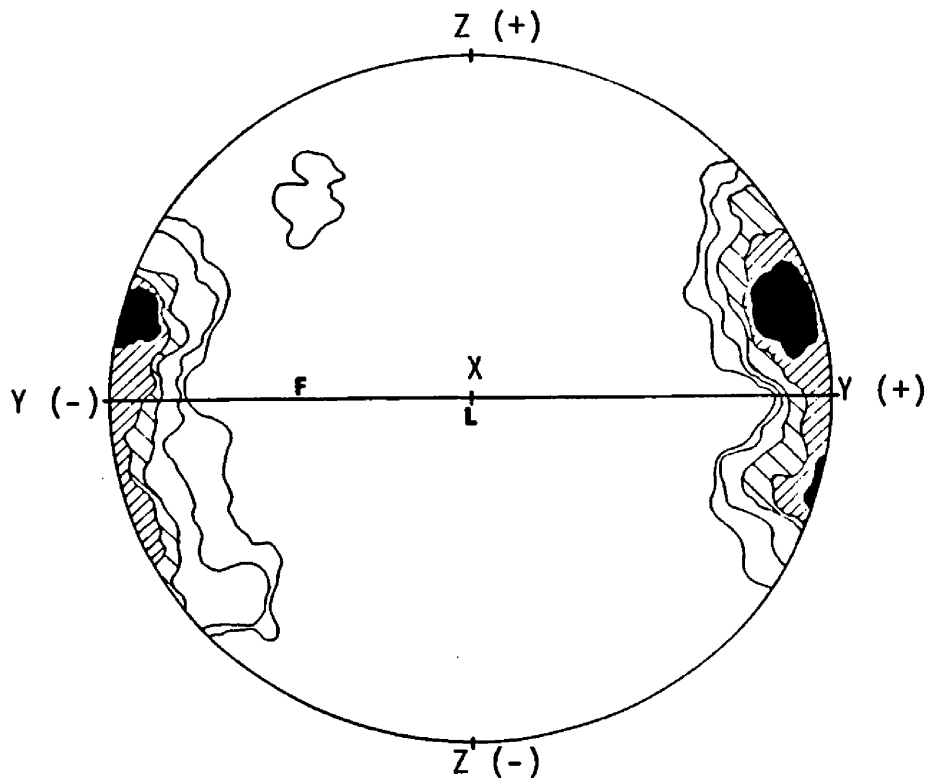


Figure 16. Orientation diagram for weakly mylonitic sample RL-19b; 250 quartz [0001]. Contours are 8, 6, 4, 2 and 1%.

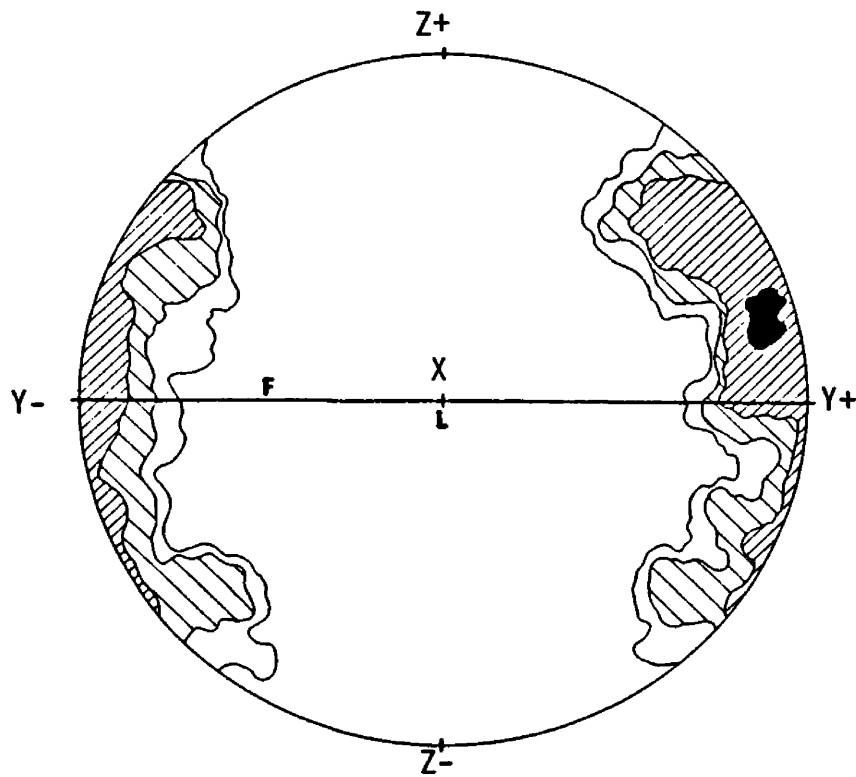


Figure 17. Orientation diagram for strongly mylonitic sample RL-B; 250 quartz [0001]. Contours are 6, 4, 2 and 1%.

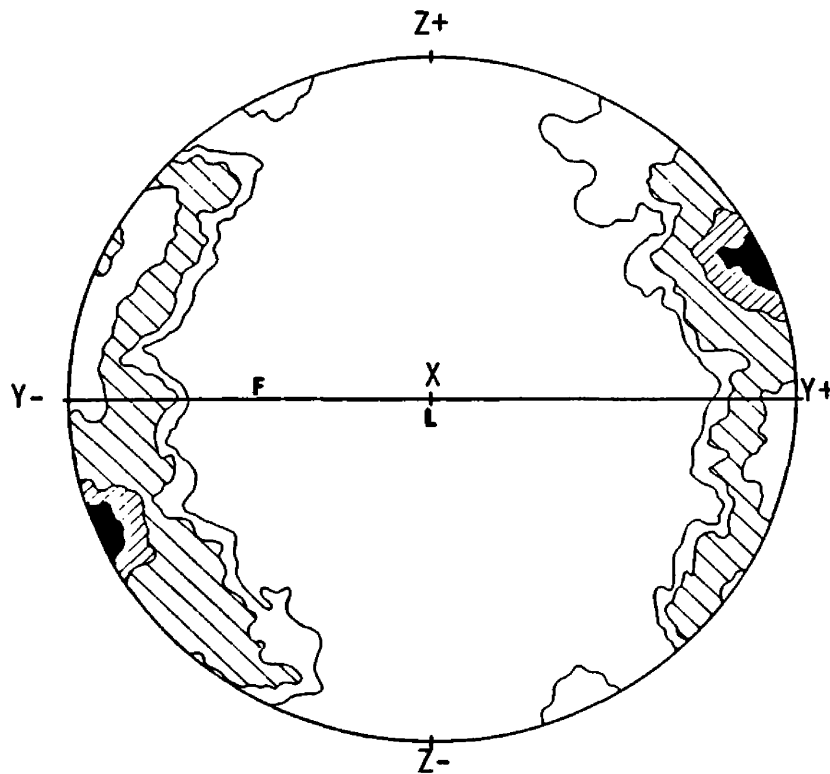


Figure 18. Orientation diagram for strongly mylonitic sample C-4b; 274 quartz [0001]. Contours are 6, 4, 2, and 1%.

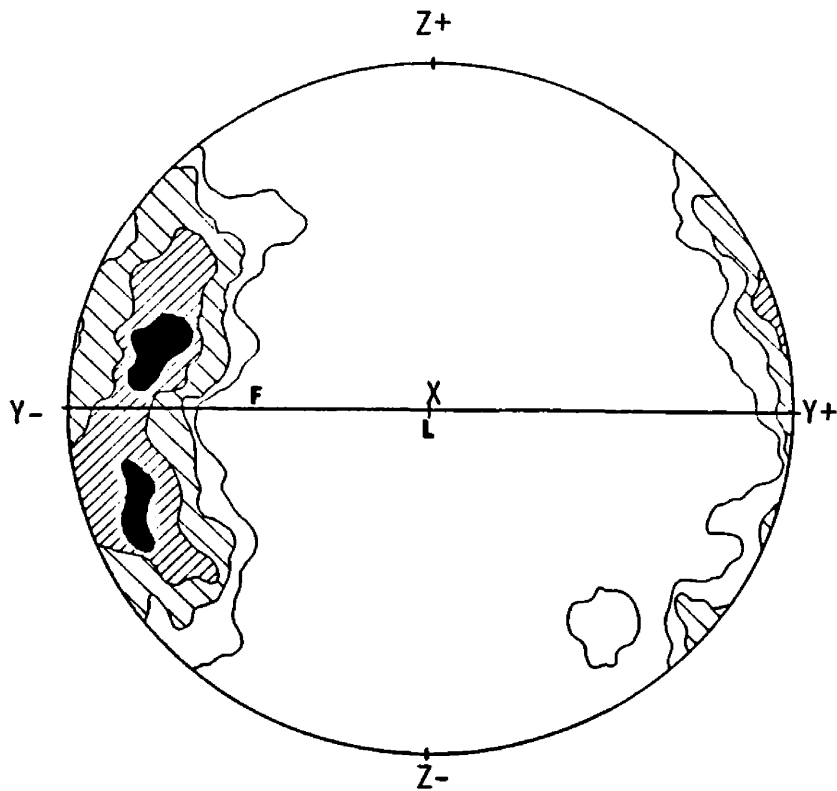


Figure 19. Orientation diagram for strongly mylonitic "black mylonite" sample RL-26b; 250 quartz [0001]. Contours are 6, 4, 2, and 1%.

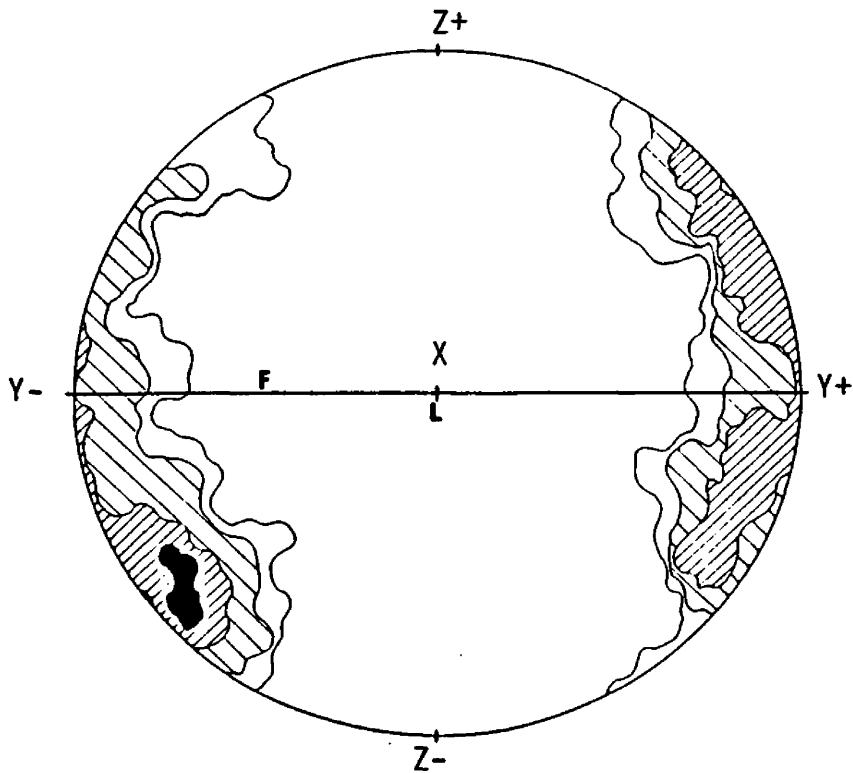


Figure 20. Orientation diagram for strongly mylonitic "white mylonite" sample RL-30b; 250 quartz [0001]. Contours are 6, 4, 2 and 1%.

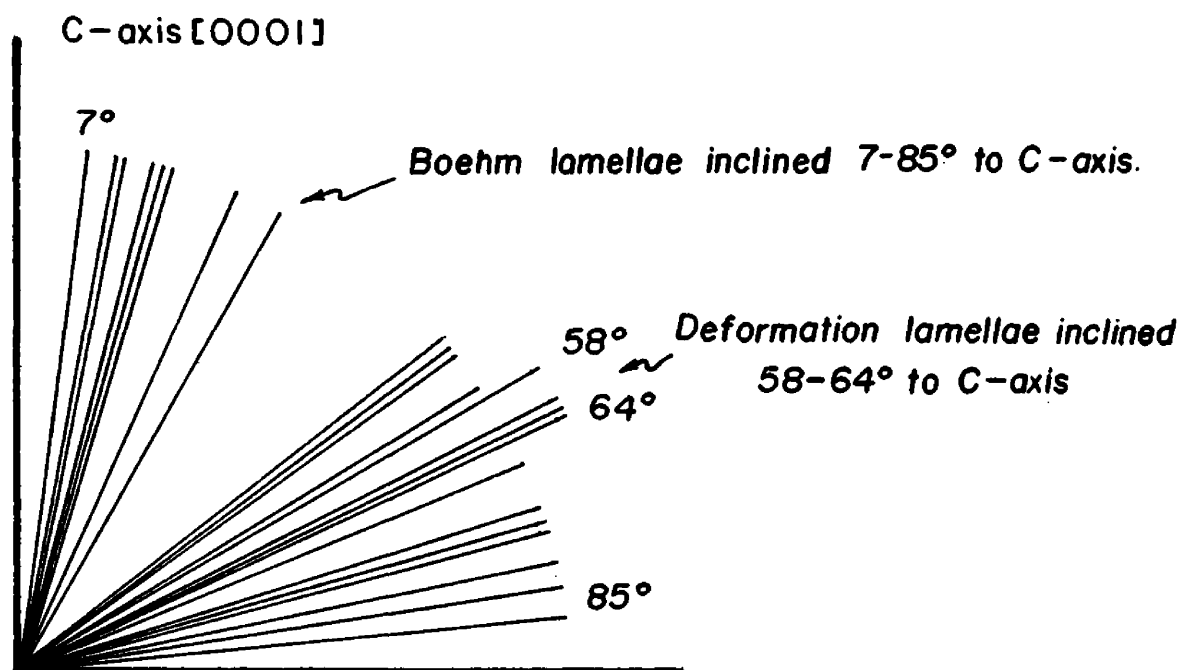


Figure 21. Orientation of "Boehm" and deformation lamellae planes relative to quartz C-axis. (See text)

Deformation lamellae. Although quartz deformation lamellae have been used by a number of workers to determine stress and movement (see for example Carter and Raleigh, 1969), too few were observed in thin sections prepared in this study for such analysis. However, two distinct types were observed. Planar bubble trains, probably Boehm Lamellae (Hobbs, et al, 1976, pg. 99), occur in but a few grains in mylonitic and nonmylonitic samples. These occur singly or in subparallel sets, commonly are discontinuous and roughly normal to extinction bands within the grain. Faint, closely spaced parallel deformation lamellae (Plate 15) occur in several grains in two samples (RL-19b and GS-4a). Figure 21 shows the orientation of "Boehm" Lamellae in 14 grains and deformation lamellae in 2 grains relative to the C-axis in sample RL-19b. The



Plate 15. Photomicrograph of deformation lamellae in quartz, sample RL-19. Field of view (long dimension) is 0.9 mm.

Boehm Lamellae are irrational and varied in inclination from 7 to 85 degrees relative to the C-axis. Deformation lamellae in the two other grains were inclined between 58 and 64 degrees to the C-axis. There is no apparent, consistent relationship between lamellae planes and the C-axis and since lamellae are rare in these rocks no further study of them was conducted.

Biotite Orientation

The orientation of poles to biotite $\{001\}$ in the nonmylonitic sample studied is random (see Fig. 22). Although mesoscopically visible subparallel biotite or biotite-rich layers define a weak foliation in some nonmylonitic samples, no preferred orientation or foliation defined by biotite is apparent in this sample. Therefore, the biotite subfabric symmetry of this sample is statistically spherical.

Poles to biotite $\{001\}$ in the weakly mylonitic sample (Fig. 23) display a maxima and girdle pattern symmetric about the XZ plane with Y corresponding to the girdle axis. Biotite subfabric symmetry is orthorhombic in the weakly mylonitic sample. A similar pattern of preferred orientation exists for the strongly mylonitic sample (Fig. 24). Although poles to biotite $\{001\}$ show nearly axial symmetry in this diagram, consideration of the weak XZ girdle renders the symmetry orthorhombic. Obviously, biotite shows a strong preferred orientation in mylonitic rocks with $\{001\}$ subparallel to foliation, the XY plane.

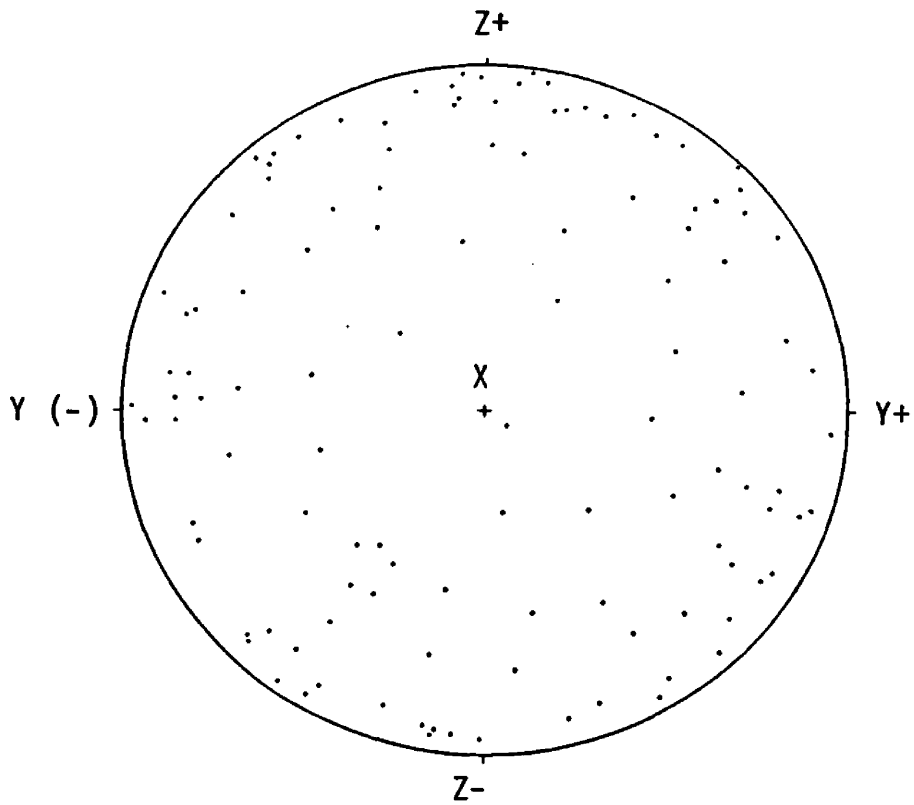


Figure 22. Orientation diagram for nonmylonitic sample RL-1b; 115 poles to biotite {001}.

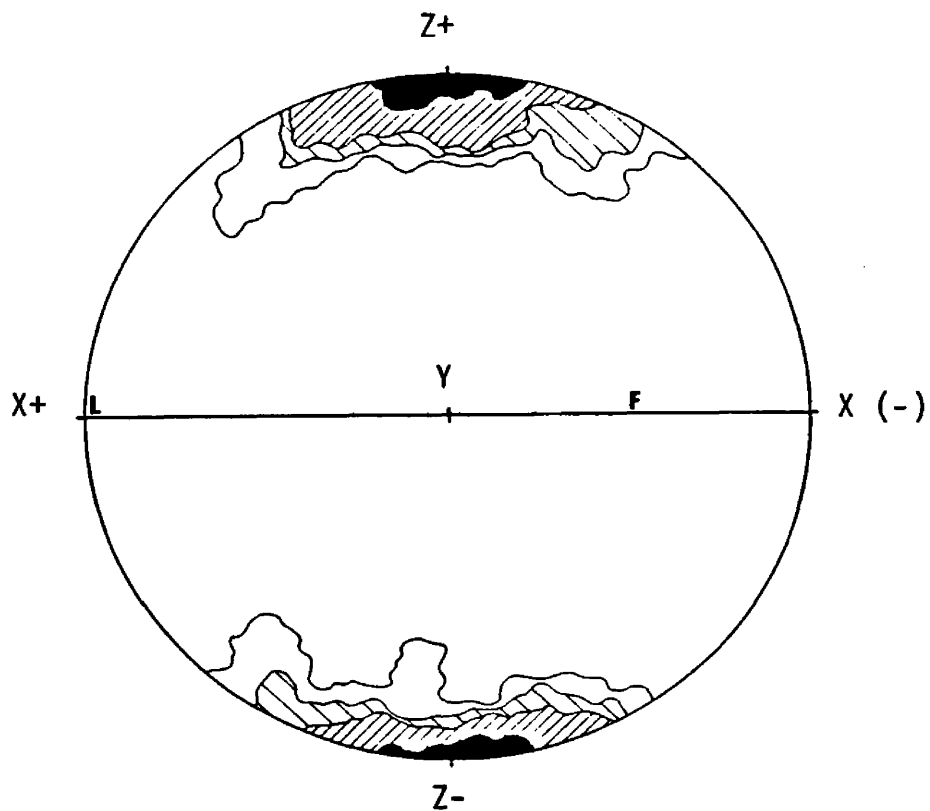


Figure 23. Orientation diagram for weakly mylonitic sample RL-13a; 150 poles to biotite {001}. Contours are 8, 6, 4, and 2%.

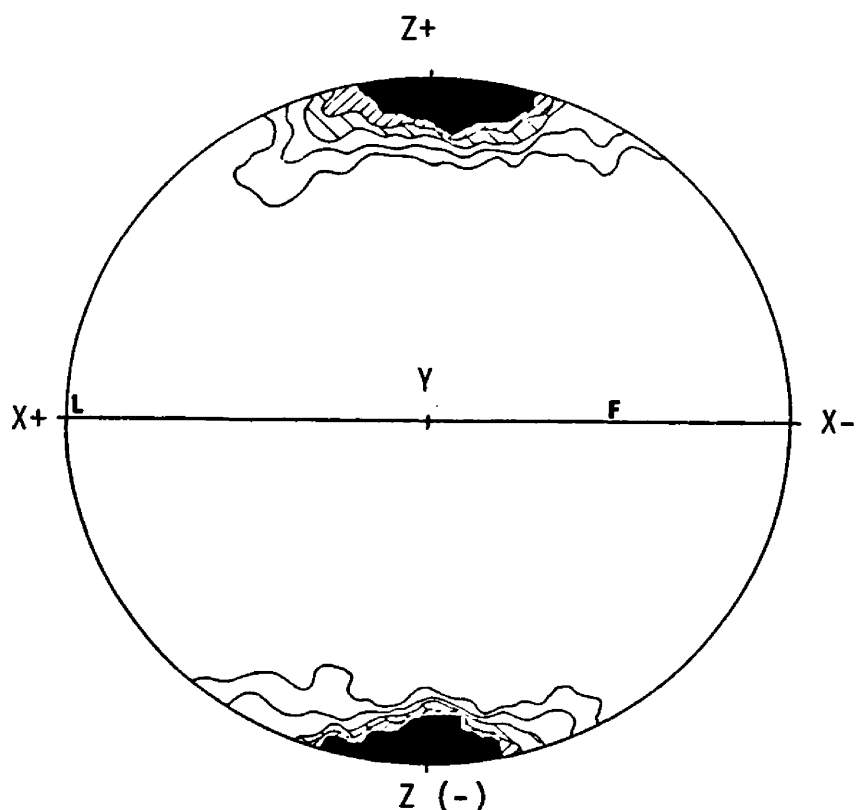


Figure 24. Orientation diagram for strongly mylonitic sample RL-A; 150 poles to biotite {001}. Contours are 10, 8, 6, 4, and 2%.

Fabric Symmetry from Microscopic and Mesoscopic Elements

The symmetry of the fabric is given by the symmetry elements (i.e. axes, planes, translation lines etc.) that are common to the symmetries of the subfabrics for the various kinds of fabric elements being taken into account (Paterson and Weiss, 1961). In this study the fabric elements include mesoscopic foliation and lineation, and microscopic preferred orientation the quartz c-axes and poles to biotite {001}. In the mylonitic zone the symmetries of the subfabrics are either axial (foliation and lineation) or nearly so (biotite) or orthorhombic (quartz-c-axes and biotite {001}). Because the fabric cannot have symmetry higher than any of its subfabrics, and symmetry elements not present in

all subfabrics are not symmetry elements of the fabric, the symmetry for the fabric in the mylonitic zone is orthorhombic. Figure 25 diagrammatically illustrates the symmetry elements common to the fabric elements measured in this study.

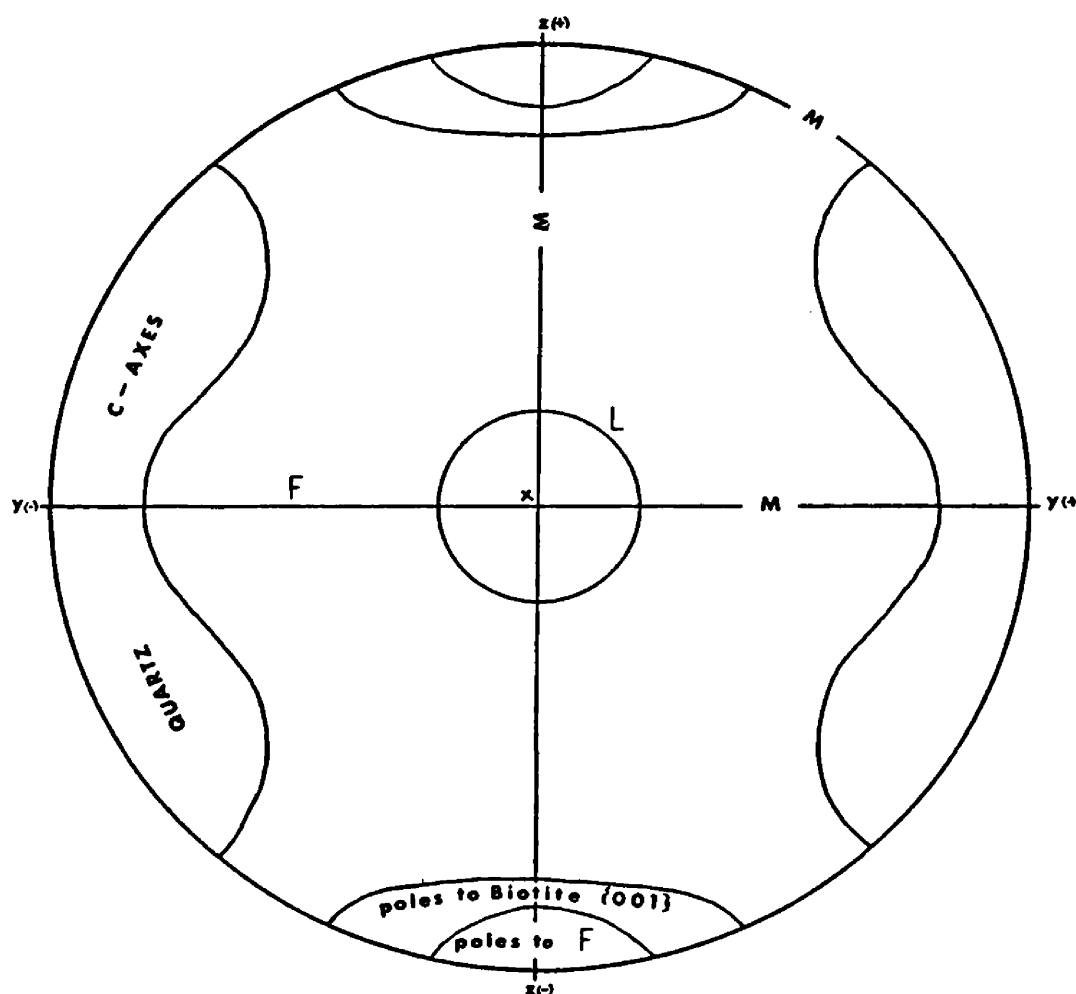


Figure 25. Combined symmetry elements from quartz [0001], biotite {001}, poles to foliation, and lineations. Fabric symmetry considering these elements is orthorhombic. M = minor plane, F = foliation, L = lination, X,Y,Z = fabric axes.

The fabric symmetry for nonmylonitic rocks, considering the fabric elements foliation, quartz c-axis and biotite {001} orientation, would approach spherical for nonfoliated areas and likely be orthorhombic for foliated areas. However, in undeformed granitic rocks showing little preferred orientation, fabric symmetry is of questionable value. Regardless of the original fabric symmetry, the resultant fabric symmetry in the mylonitic zone is orthorhombic and evolved from dominantly isotropic rock with the development of fabric elements during deformation. The fabric elements and therefore the symmetry has been acquired.

CHAPTER VI

DYNAMIC INTERPRETATION

General Statement

Evolution of the mylonitic zone viewed in terms of a model, helps to visualize the progressive development of mylonitic foliation and lineation from originally isotropic rocks of the Idaho batholith. Although several models exist (discussed below) or might be imagined, consideration of Hyndman's (1980) Bitterroot dome - Sapphire tectonic block model with fabric development resulting from progressive offloading of the Sapphire tectonic block best serves this purpose. Inherent to this model are conclusions relating to the amount and direction of movement, the superposition of brittle deformation features on ductile deformation features resulting from changing conditions during movement, and isostatic rise of the Bitterroot dome in response to progressive offloading of the Sapphire tectonic block. Evidence presented below is compatible with these conclusions and the model but is not restricted to it.

Physical Conditions in the Mylonitic Zone

Regional metamorphism, up to sillimanite-orthoclase-grade, and emplacement of the Idaho batholith preceded formation of the mylonitic zone (Chase, 1977). Pressure-temperature estimates from mineral assemblages within the metamorphic rocks, and granites of the Idaho batholith,

range from about 450°C - 700°C (Chase, 1977) and 3.5 kb - 6.7 kb (Hyndman, 1980). This, in addition to the estimated 17 km thickness of the Belt section in the Sapphire Tectonic block and the ductile fabric characteristics in the mylonitic zone, all suggest that high-temperature-high-pressure conditions existed prior to and during early stages of formation of the mylonitic zone. Temperature must have remained high for a long period of time because late, weakly oriented potassium-feldspar megacrysts appear relatively undeformed, apparently cut the fabric in black mylonite and are being replaced by myrmekite. The potassium feldspar-myrmekite assemblage is common in late-magmatic indigenous microveins (Hibbard, 1980). Also, andalusite and cordierite in the metamorphic rocks (Cheney, 1975) indicate high-temperature conditions but superposition of more-brittle "slickensided" shear surfaces on ductile fabrics suggest that conditions changed during evolution of the zone to a shallower brittle environment.

Fabric Development

With the model in mind, and realization that conditions must have changed dramatically during formation of the mylonite zone, the progressive development of mylonitic fabric from an essentially isotropic granite-granodiorite protolith, might well be anticipated. Figure 26 shows the paragenetic sequence for minerals involved in mylonitization and Figure 27 summarizes changes in the fabric and relates them to proposed tectonic events leading to formation of the mylonitic zone and the microstructural characteristics occurring in it.

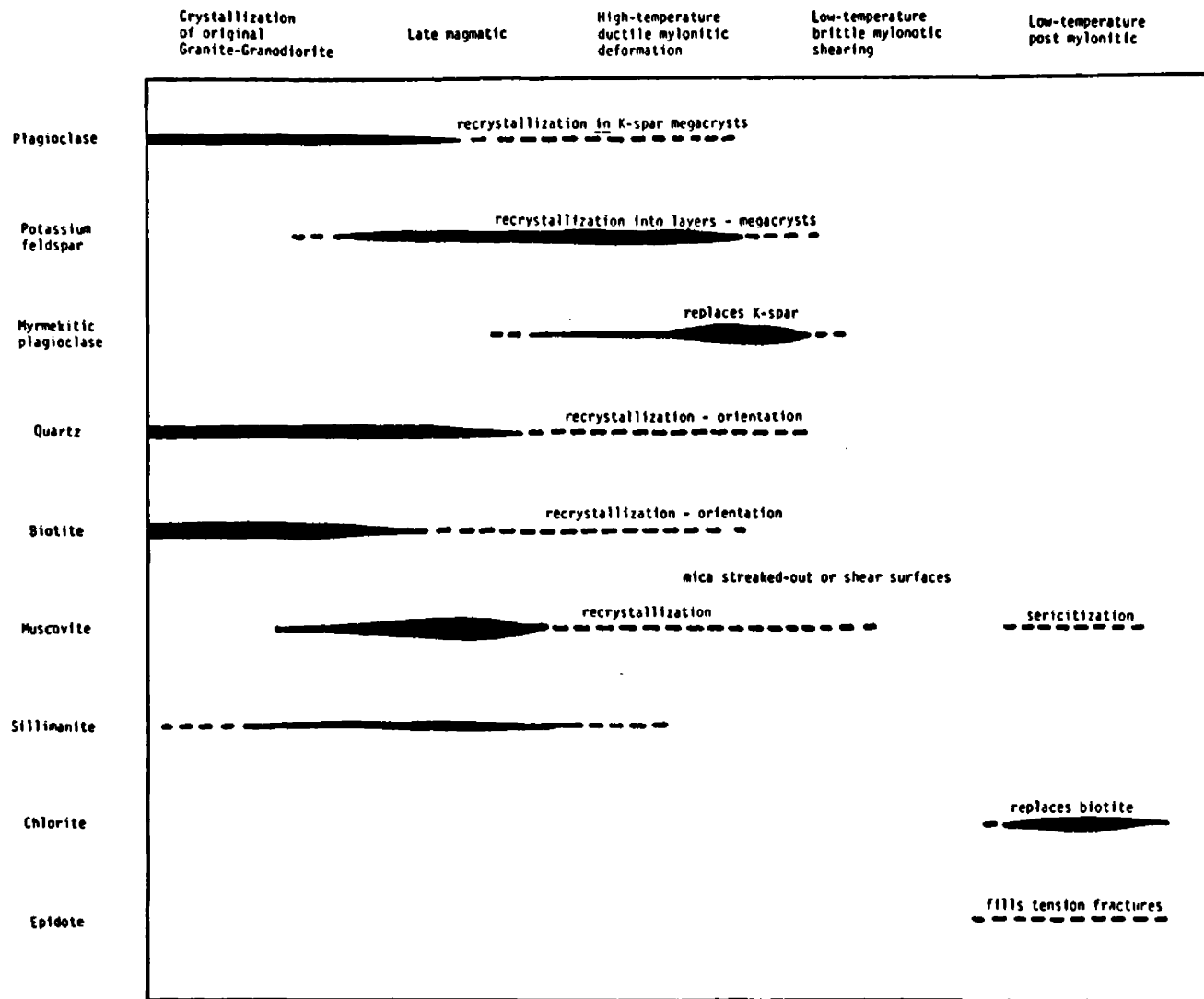


Figure 26. Paragenetic sequence for minerals in the mylonitic zone. Periods of growth indicated by width and length of line.

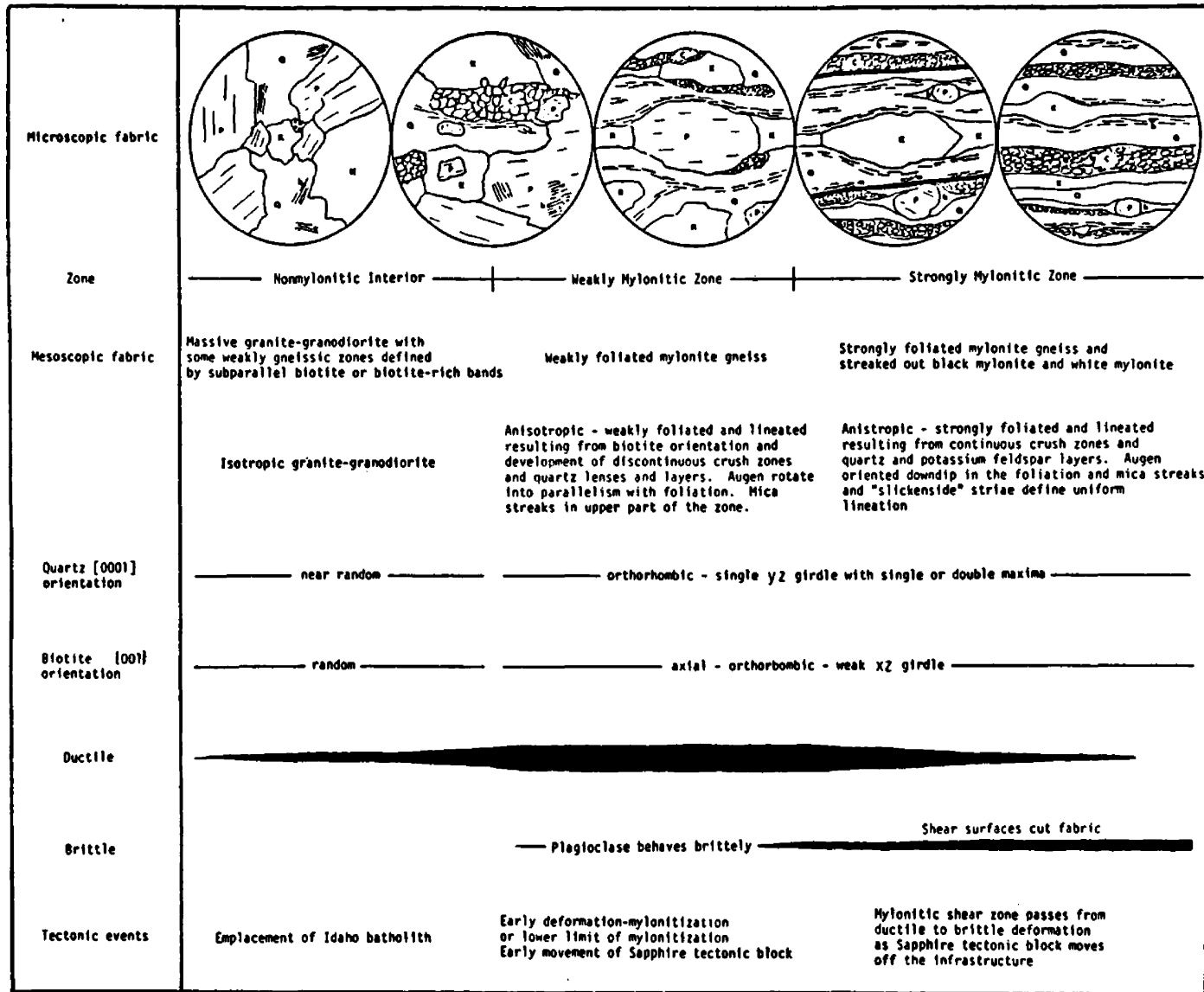


Figure 27. Summary of fabric development.

Evident both mesoscopically and microscopically, is the increasing degree of deformation upward toward the detachment surface. Intra-granular deformation in individual minerals evidenced by strain shadows, bent, broken or displaced twin lamellae and flattened grains increases upward through the mylonitic zone. However, it is the intergranular development of matrix material such as quartz-feldspar-rich crush layers, layers and rods of clean quartz and/or potassium feldspar, and parallelism of biotite that best reveals the increasing degree of deformation. Certainly the most obvious change in the mesoscopic fabric is the development of mylonitic foliation and lineation. Obviously, components of the matrix define the foliation and enhance it as more matrix is generated.

Individual minerals either recrystallized or deformed brittlely and/or ductilely and roughly behave according to Higgins' (1971) "cataclastic" reaction series. Quartz and mica deform easily, and in part define the foliation which suggests that orientation resulted from recrystallization during deformation (Hyndman, 1972). Quartz [0001] and biotite {001} acquire a strong preferred orientation and under the proposed conditions, recrystallization rather than rotation or crystallographic slip is the probable orienting mechanism (Hobbs and others, 1976). In marked contrast to quartz and biotite, plagioclase deformed either ductilely, or form bent or kinked twin lamellae, or commonly in a more brittle fashion with little or no recrystallization. Rigid-body rotation was probably responsible for orienting augen downdip in the foliation. In more deformed zones plagioclase is commonly round, has rough edges, and pressure shadows contain chips plucked from the grain suggesting that

plagioclase was rolled and granulated. Potassium feldspar augen also may have rotated into the foliation and some grains appear stretched and/or broken into smaller grains. Isolated microcline grid twins appear in deformed grains and layers with patchy undulatory extinction. However, the appearance of potassium feldspar in pressure shadows, in layers and lenses parallel to foliation and as weakly oriented, relatively undeformed megacrysts suggests that recrystallization partially controlled its orientation and location in the fabric. Evidently, conditions favorable for growth of potassium feldspar outlasted much of the deformation as large megacrysts appear to cut strongly deformed fabric, particularly in the black mylonite. However, some in turn are cut by crush layers. Also, some megacrysts enclose broken and annealed plagioclase grains (see Plate 11). Myrmekite, common in the crush zones and typically replacing potassium feldspar megacrysts and layers appears relatively undeformed and from these relationships apparently formed late as well. Conditions for crystallization of muscovite also must have outlasted much of the deformation. Muscovite occurs as thin stringers along shear surfaces, replaces some biotite and larger grains cut the fabric and earlier crystals. Some muscovite flakes are kinked or bent whereas others have recrystallized into polygonal arcs. The degree of deformation and orientation of late minerals may have depended on whether they grew in kinematically "active" or "dead" parts of the mylonitic zone. Chlorite, epidote, and sericite are retrograde minerals unrelated to the mylonitic deformation.

In the nonmylonitic interior, undulatory quartz with perhaps a weak preferred orientation of c-axes, is the only common indication of strain.

With the transition to weakly mylonitic rocks, undeformed layers or small boudins appear and are enclosed by sheared rock. In thin section the transition is marked by the appearance of discontinuous crush layers and orientation of biotite defining a weak foliation.

Further development of the crush layers, biotite orientation, segregation of quartz into discontinuous clean layers, and rotation of feldspar augen into the weak foliation, give the weakly mylonitic zone its characteristic mylonite gneiss fabric. Although the matrix is only weakly developed and not necessarily penetrative on the scale of a thin section, rocks in this zone are relatively homogeneous throughout the zone and display a ductile matrix which flowed around closely packed feldspar augen. Deformation in this zone might be related to either the early stages of movement, or the lower limit of deformation within the whole mylonitic zone.

In the strongly mylonitic zone, intragranular deformation and intergranular matrix development becomes more pronounced and penetrative on all scales. In thin section, virtually all minerals appear more deformed. Undulatory extinction, common in plagioclase, most potassium feldspar, and especially quartz is greater than in lower zones. The ductile matrix is more continuous, laminated, and flows around or cuts the larger augen. A general finer grain size results from more widely spaced feldspar augen suspended in fine matrix material in mylonite gneiss, and the increased presence of the fine-grained, streaked-out, black mylonite and white mylonite layers. Strain clearly is greater in this zone but the fabric for the zone as a whole is less homogeneous,

suggesting that the strain was more variable. Presumably, deformation became more localized (possibly due to work hardening?) and intense closer to the suprastructure detachment surface, forming stronger mylonitic fabrics and zones.

The black mylonite layers are essentially fine-grained versions of typical mylonite gneiss and resemble "ductile deformation zones" of Mitra (1978). They are localized zones of intense strain and deformation, and because they commonly cut the mylonite gneiss fabric at low angles, they are, at least in some cases, later than the surrounding rock. Localized differential movement within the mylonitic zone (i.e. variable strain rate through the zone) probably best explains their existence. However, as suggested by the low-angle, commonly shallower dip, and cross-cutting relationships, the attitude of the mylonitic zone may have changed periodically by uplift or isostatic rise of the infrastructure. In this case the gravity potential may have increased slightly thereby accelerating movement. If the white mylonites are sheared pegmatites, which were injected during deformation, they may have localized strain.

Superimposed on mylonitic fabrics within the strongly mylonitic zone and the upper part of the weakly mylonitic zone, and crossing the whole crest and eastern flank of the dome, are the closely spaced, nearly planar shear surfaces containing consistently oriented mica streak and "slickenside" laminae. These occur late in the deformation sequence for several reasons. They closely parallel other planar fabric features such as the crush layers, but cut through them, offset augen (see Plate 9) and must have formed under different conditions. Although these brittle

phenomena conceivably could form because of an increased strain rate, it seems unlikely they would be preserved at the high temperatures present during the formation of ductile fabric features.

Deformation resulting in formation of the mylonitic zone, its textural zones, rock types, and microstructures might be viewed as continuous, sporadic or a two-event process, ductile followed by brittle. The degree of deformation increases upward through the zone and individual minerals behaved differently. However, it seems clear that most of the fabric characteristics, evolved under deep-seated ductile conditions. The forces involved were constant in direction although probably not in magnitude.

Implications of Preferred Orientation and Symmetry

Clearly the mylonitic foliation and lineation, and the dimensional and crystallographic preferred orientation encountered in the mylonitic zone are acquired characteristics not found in the nonmylonitic interior. The fabric developed from essentially isotropic protolith, and no fabric elements were inherited. Therefore, mylonitic foliation, lineation and the microstructural characteristics found in the mylonitic zone may be considered "kinematically active", and the result of deformation.

Each fabric element and its symmetry considered alone reveal little about the kinematic framework or movement picture. However, together with macroscopic structural features a clearer picture evolves. The preferred orientation pattern of biotite is axial to orthorhombic, reflecting mesoscopic foliation and biotite wrapping around augen.

Measurement of biotite orientation offers little information that could not be obtained by simply measuring mesoscopic foliation. Besides its symmetry, it does however give information relating to the time sequence in which mylonitic foliation appeared in the fabric. Timing and symmetry are also the most important results offered in measuring quartz c-axis orientation and like biotite, quartz apparently oriented early in the deformation sequence, shows orthorhombic patterns, and does not change even in zones of high strain. For instance, compare the diagram for weakly mylonitic sample (Fig. 14), with the diagram for black mylonite sample (Fig. 19). With reservation, Turner and Weiss (1963) suggest "that syntectonic recrystallization of quartz yields patterns whose symmetry approximates that of the stress system", and "the three mutually perpendicular directions of intersection of the planes of near-symmetry could be equated with the axes of principal stress σ_1 , σ_2 , and σ_3 ". Feldspar augen define a weak lineation in mylonitic zones. Since feldspar grains and "phenocrysts" in nonmylonitic rocks are randomly oriented, they either rotated or grew into their present orientation. Foliation wraps around the augen suggesting that most were present prior to deformation. Feldspar augen orientation was not measured directly but their general linear arrangement, microscopic extension fractures, and offset suggest stretching and shearing down-dip in the foliation. Considering the "slickenside" and mica-streak orientation within the mylonitic foliation, at least the line and plane of moment can be determined. The symmetry of these features is axial. Together, these elements define a homotactic orthorhombic fabric.

In this fabric, orthorhombic symmetry, preferred mineral orientation, mylonitic foliation, and slickenside orientation can reasonably be correlated with an orthorhombic system of strain and perhaps stress (i.e., $Z = \sigma_1$, $Y = \sigma_2$, $X = \sigma_3$, of the fabric axes). However, the movement picture cannot be deduced from combination of just these elements alone, especially in orthorhombic fabrics. Chase's (1968) orientation diagrams for similar rocks and zones showed monoclinic to orthorhombic symmetry, and on symmetry grounds for monoclinic fabrics and lineations, he could identify the direction of greatest differential displacement. If Y were correlated with a rotation axis as suggested by asymmetric folds, rolled augen, and rotation of fold axes in metamorphic rocks farther north (Chase, 1977), then the fabric symmetry would be reduced to monoclinic. Monoclinic symmetry also would agree with a simple shear model of deformation and displacement (Turner and Weiss, 1962). So, although the direction of movement seems apparent considering fold asymmetry, infrastructure-superstructure relationships, and the slickenside orientation, it cannot be determined from the orthorhombic fabric symmetry of rocks in this study.

Movement Picture

The fabric, its symmetry and microstructural characteristics, are consistent with a model involving unidirectional, progressive or sporadic, deformation from ductile to brittle conditions. Correlating fabric axes with axes of stress and strain is speculative but assigning a movement direction is not. It is not clear from the fabric alone whether pure shear (orthorhombic) or simple shear (monoclinic) was the dominant type

of strain. Nor is the amount of translation through the zone apparent from the fabric.

Hyndman (1980) proposed 60 km of movement. Minimum estimates of eastward movement derived from rotated folds in metamorphic rocks in the mylonitic zone (Hyndman and others, 1975; Chase, 1977), and movement on thrusts in the Sapphire tectonic block (Csejtey, 1963) are 15 km and 25 km respectively. Acceptance of the genetic relationship between the Bitterroot dome, the mylonitic zone and Sapphire tectonic block implies that the distance across the dome (the area unloaded) should approximate the eastward transport of the Sapphire block (Hyndman, 1980). Slip would occur on innumerable shear surfaces through the average 1 km thick mylonitic zone. Obviously, more translation occurred in some zones than others. In this model, the allochthonous Sapphire tectonic block suprastructure detached and slid 60 km off the infrastructure, forming the intervening mylonitic zone, and the Bitterroot dome is the result of isostatic recovery.

A broad macroscopic flexure or diapiric uplift along a north-trending axis as suggested by Chase (1973), possibly against an autochthonous superstructure (Chase, in Clark, 1979, p. 11), could result in shearing along the infrastructure-suprastructure boundary. This would lead to formation of the zone of mylonitization and the Bitterroot dome. However, the unidirectional "slickenside" striae and asymmetric fabric which is strongest along the Bitterroot front, suggests that movement was unidirectional across the whole dome. Rise of a mobile infrastructure presumably would result in a fabric with a radial arrangement of "slickensides" or other linear features.

CHAPTER VII

COMPARISON WITH SIMILAR COMPLEXES AND MYLONITE ZONES

Microscopic, mesoscopic, and macroscopic elements evident for the Bitterroot dome, Sapphire tectonic block and mylonitic zone are common to Cordilleran metamorphic core complexes (Coney, 1973) in general. For a review of these complexes see Coney (1980) and Crittenden (1980). Microfabric characteristics found in the zone of mylonitization are also common to other mylonite zones generated under similar conditions. Although the cordilleran metamorphic core complexes differ somewhat in detail, kinematic history, and age, all possess at least three common macroscopic elements or zones:

- 1) an infrastructure or "core zone" of some workers, where sillimanite-zone regional metamorphic rocks and/or granitic plutons commonly display ductile deformation structures (often polyphase) developed under high-temperature, deep-seated ductile conditions and are presently exposed as an elliptical uplift or dome,
- 2) an overlying or adjacent unmetamorphosed to low-grade suprastructure, where rocks of variable composition display open folds, thrusts and listric normal faults developed under shallow brittle conditions, and
- 3) an intervening gently-dipping lineated and foliated mylonitic shear zone from several meters to over a kilometer thick, commonly exhibiting characteristics of both brittle and ductile deformation, high strain, and steep metamorphic gradient, and characteristically

more-intense development on one side of the infrastructure than the other.

These macroscopic elements correspond to the Bitterroot dome, Sapphire tectonic block and zone of mylonitization, regardless of any model of inferred movement. However, the remarkable commonality between complexes and surrounding terrane suggests that many may have formed under similar conditions and play a major role in the geologic evolution of the Cordillera.

Mesoscopic and microscopic fabric characteristics encountered in the zone of mylonitization along the Bitterroot front closely resemble those found in the mylonitic shear zones (Abscherungszone, decollement, mylonite front, detachment fault, etc.) of other complexes. They are characterized by the contrasting ductile and brittle behavior of their mineral components (Davis and others, 1980) and fabric elements in general, although this aspect seems unrecognized by many workers. Common conclusions regarding these zones include the following: 1) The mylonitic foliation and lineation are superimposed on earlier fabrics and diminish downward into either undeformed or earlier metamorphic fabrics. 2) Strain is extreme with maximum shortening normal to foliation and maximum extension parallel to the lineation, which commonly trends normal to the axis of the dome. 3) Surfaces (late shear surfaces in the present study) parallel the mylonitic foliation and contain unidirectional mineral and "slickenside" striae oriented in the direction of movement. 4) The zone is a structural boundary but not a discrete fault surface. 5) Conditions were sufficient to cause quartz to behave

ductilely or recrystallize producing a preferred orientation of c-axes. 6) Regionally constant stress fields evidently existed for long periods of time, as shallow brittle structures are superimposed on deep-seated ductile structures. 7) Brecciation, chloritic alteration, and an abrupt change in metamorphic grade mark the top of the zone. 8) The zones formed at shallow dips and were later arched or uplifted to their present angle of dip of less than 30° . Mylonitic shear zones are, of course, not identical from complex to complex but those differences that exist can commonly be attributed to either the variable thickness or to whether the zone has been subdivided into ductile vs. brittle parts. Differences in original protolith also may have influenced fabric development. Nonetheless, the fabric in these zones is remarkably similar.

Quartz orientation diagrams commonly display orthorhombic or nearly orthorhombic symmetry in mylonitic rocks (Turner and Weiss, 1963, p. 432) suggesting that the stress system is also orthorhombic. Although the details of the microfabric diagrams differ (i.e., cross-girdle vs. single girdle with single or double maxima), the symmetry remains essentially orthorhombic. The quartz orientation diagrams in this study are orthorhombic as are those from similar mylonite zones in complexes studied by Snoke (1980) and Compton (1980). Snoke's (1980, pg. 310) diagrams are virtually identical to my diagrams. Flattening or shortening normal to the mylonitic foliation and extension parallel to the lineation seems certain in the mylonitic shear zones. The orthorhombic symmetry of the quartz c-axis microfabric (and possibly the whole fabric in this study)

based on symmetry arguments alone suggests that progressive pure shear was the dominant deformational mechanism (see Johnson, 1967, pg. 247). Compton (1980) favors a model relying on progressive pure shear or flattening for mylonitic rocks in the Raft River Mountains in Utah. However progressive simple shear (for example, Escher and Watterson, 1974) and apparently nearly analogous quartz microfabrics found in "tectonites" deformed by progressive simple shear (Hara and others, 1973), suggested to Snoke (1980) that possibly two tectonic models are consistent with the data, and elements of both models probably were operative during the deformation. Such is apparently the situation for the Woodruffe thrust, a ductile mylonite zone in Australia, where inhomogeneous forms of both progressive pure shear and progressive simple shear played a role (Bell, 1978). Pure shear dominated initially but gradually gave way to simple shear leading eventually to brittle rupture and detachment. Consideration of the regional geology, and the mesoscopic and microscopic elements measured in this study, a model involving a similar deformation path seems appropriate for evolution of the mylonitic zone.

The mylonitic microfabric characteristics common to mylonitic shear zones in Cordilleran metamorphic core complexes, are also common to mylonite zones formed under similar physical conditions in general. As expected, the origin of mylonitic rocks is controversial and certainly described as different for various areas, but most possess the characteristic foliation, lineation, and contrasting ductile-brittle features. Structural analysis of various mesoscopic and microscopic elements is the common approach to dealing with these zones, and symmetry combined with elements at all scales best serves interpretation.

CHAPTER VIII

CONCLUSIONS

A model designed to explain the origin of the mylonitic rocks forming the gently-dipping Bitterroot front, must account for mesoscopic and microscopic fabric characteristics evident within the zone as well as its position relative to adjacent terranes of divergent rock types, metamorphic grade and structural style. Information collected and analyzed for this study was not intended to prove or disprove existing models but rather to provide information on fabric development and mineral orientation within the mylonitic zone, information critical to any theory regarding its origin. Conclusions based on data obtained from this study are compatible with a model involving progressive development of mylonitic fabric from essentially isotropic protolith, with fabric development advancing from deep-seated ductile conditions to shallow brittle shearing. A model involving initial diapiric rise of the Bitterroot dome infrastructure from deeper levels to its present level of exposure is consistent with my data but would only explain the mylonitic zone along the Bitterroot front. A model with a broader perspective, and recognition of the importance of the following is also consistent with the following data: 1) A penetrative mylonitic foliation with unidirectional mineral streaking and "slickenside" lineation crosses the dome, is strongest on the eastern flank of the dome, fades downward and westward, and forms the infrastructure-suprastructure boundary.

2) The Bitterroot dome is matched in its dimensions by the Sapphire tectonic block. 3) The inferred depth and time of formation of the mylonitic zone is compatible with the thickness and time of thrusting in the Sapphire block. These are key factors in Hyndman's (1980) model of detachment of the Sapphire tectonic block off the infrastructure with the Bitterroot dome being the physiographic result of offloading and isostatic recovery.

In any event, certain things seem clear. The Bitterroot Range has risen with respect to the Sapphire Range. The fabric in the mylonitic zone forming the Bitterroot front developed by progressive mylonitization of originally isotropic rocks of the Idaho batholith. Conditions changed during its development from deep-seated, ductile flow to shallow, brittle shearing. Discrete, penetrative shear surfaces containing unidirectionally oriented mineral streak and "slickenside" striae indicate down-dip shear occurred along the foliation late in the deformation sequence under more-brittle conditions. Ductile fabrics and textures suggest flattening normal to foliation, extension parallel to lineation and probable translation down-dip as well. Crystallographic preferred orientation of quartz [0001] and biotite {001} in mylonitic rocks remains constant regardless of the degree of strain. Strain increases upward through the zone of mylonitization. Temperature was high during most of the deformation, allowing growth of sillimanite (in the nonmylonitic interior and weakly mylonitic zone), potassium feldspar megacrysts, myrmekite, and muscovite. Also andalusite and cordierite occur in the metamorphic rocks north of the study area. Deformation, at the macroscopic scale may be

homogeneous but is obviously inhomogeneous mesoscopically. Black mylonites and white mylonites are local zones of intense strain.

Perhaps less clear is the type and amount of shear involved in the deformation. The orthorhombic symmetry of the microfabric suggests pure shear. However, simple shear clearly was an important mechanism. Consideration of the steep metamorphic gradient between the infrastructure and suprastructure in the mylonitic zone, and the shear surfaces, mineral streak and "slickenside" lineations within this zone, indicate that deformation by a simple-shear mechanism was dominant during at least the later stages of formation of the zone.

Fabric development within the mylonitic zone can reasonably be envisioned as the result of progressive offloading of the Sapphire tectonic block closely following the model proposed by Hyndman (1980). Considering the symmetry, inhomogeneous (?) pure shear likely dominated initially resulting in development of mylonitic foliation and lineation in weakly mylonitic rocks. As movement of the block began, pure shear gradually gave way to inhomogeneous simple shear producing further development of the ductile mylonitic fabric. Strain was inhomogeneous, resulting in varied mylonite gneiss fabrics. As the thin tail end of the block passed overhead, conditions changed dramatically leading ultimately to brittle rupture and further detachment on individual shear surfaces in the upper part of the zone. The present average 20° angle of dip of the mylonite zone resulted from isostatic recovery.

REFERENCES CITED

- Anderson, R.E., 1959, Geology of lower Bass Creek Canyon, Bitterroot Range, Montana: Unpubl. M.S. thesis, University of Montana, 70 p.
- Bell, T.H., 1978, Progressive deformation and reorientation of fold axes in a ductile mylonite zone: The Woodroffe thrust: *Tectonophysics*, v. 44, p. 285-320.
- Berg, R.B., 1968, Petrology of anorthosites of the Bitterroot Range, Montana, in *Origin of anorthosites and related rocks, a symposium*: New York State Mus. and Sci. Serv. Memoir 18, p. 387-398.
- Carter, N.L. and Raleigh, C.B., 1969, Principal stress directions from plastic flow in crystals: *Geol. Soc. American Bull.*, v. 80, p. 1231-1264.
- Chase, R.B., 1961, Geology of lower Sweathouse Creek Canyon, Bitterroot Range, Montana: Unpubl. M.S. thesis, University of Montana, 83 p.
- _____, 1968, Petrology of the northeastern border zone of the Idaho batholith, Bitterroot Range, Montana: Ph.D. dissert., University of Montana, 189 p.
- _____, 1973, Petrology of the northeastern border zone of the Idaho batholith, Bitterroot Range, Montana: *Montana Bur. Mines and Geol. Memoir* 43, 28 p.
- _____, 1977, Structural evolution of the Bitterroot dome and zone of cataclasis, p. 1-24, in R.B. Chase and D.W. Hyndman, *Mylonite detachment zone, eastern flank of the Idaho batholith*: *Geol. Soc. America, Rocky Mtn. Sec. 30th Ann. Mtg. Fieldguide* No. 1.
- _____, Bickford, M.E. and Tripp, S.E., 1978, Rb-Sr and U-Pb isotopic studies of the northeastern Idaho batholith and border zone: *Geol. Soc. America Bull.* v. 89, p. 1325-1334.
- _____, and Talbot, J.L., 1973, Structural evolution of the northeastern border zone of the Idaho batholith, western Montana: *Geol. Soc. America Abst. with Prog.*, v. 5, no. 6, p. 471-472.
- Cheney, J.T., 1975, Kyanite, sillimanite, phlogopite, cordierite layers in the Bass Creek anorthosites, Bitterroot Range, Montana: *Northwest Geol.*, v. 4, p. 77-82.

- Clark, S.L., 1979, Structural and petrologic comparison of the southern Sapphire Range, Montana with the northeast border zone of the Idaho batholith: Unpubl. M.S. thesis, Western Michigan Univ., 79 p.
- Compton, R.R., 1980, Fabrics and strains in quartzites of a metamorphic core complex, Raft River Mountains, Utah: Geol. Soc. America Memoir 153, p. 385-398.
- Coney, P.J., 1973, Non-collision tectogenesis in western North America, in Tarling, D.H. and Runcorn, S.H., eds., Implications of continental drift to the earth sciences: New York, Academic Press, p. 713-727.
- _____, 1980, Cordilleran metamorphic core complexes: An overview: Geol. Soc. America Memoir 153, p. 7-31.
- Crittenden, M.D., 1980, Metamorphic core complexes of the North American Cordillera: Summary: Geol. Soc. America Memoir, 153, p. 485-490.
- Csejtey, B., 1963, Geology of the southeast flank of the Flint Creek Range, western Montana: Ph.D. dissert., Princeton Univ., 175 p.
- Davis, G.A., Anderson, J.L., Frost, E.G., and Shackelford, T.J., 1980, Mylonitization and detachment faulting in the Whipple-Buckskin-Rawhide Mountains terrane, southeastern California and western Arizona: Geol. Soc. America Memoir, 153, p. 79-129.
- Escher, A., and Watterson, J., 1974, Stretching fabrics, folds and crustal shortening: Tectonophysics, v. 32, p. 223-231.
- Greenwood, W.R. and Morrison, D.A., 1973, Reconnaissance geology of the Selway-Bitterroot Wilderness Area: Idaho Bur. Mines and Geology Pamphlet 154, 30 p.
- Groff, S.L., 1954, Petrography of the Kootenai Creek area, Bitterroot Range, Montana: Unpubl. M.A. thesis, University of Montana, 80 p.
- Hall, F.W., 1968, Bedrock geology, north half of Missoula 30-minute quadrangle: Ph.D. dissert., University of Montana.
- Hara, I., Takeda, K., and Kimura, T., 1973, Preferred lattice orientation of quartz in shear deformation: Journal of Science of the Hiroshima University, ser. C, v. 7, p. 1-10.
- Hibbard, M.J., 1980, Indigenous source of late-stage dikes and veins in granitic plutons: Econ. Geol., v. 75, p. 410-423.

- Higgins, M.E., 1971, Cataclastic rocks: U.S. Geological Survey Prof. Paper 687, 97 p.
- Hobbs, B.E., Means, W.D., and Williams, P.F., 1976, An outline of structural geology: John Wiley and Sons Inc., New York, 571 p.
- Hyndman, D.W., 1972, Petrology of igneous and metamorphic rocks: McGraw-Hill Book Co., New York, 533 p.
- _____, 1977, Mylonitic detachment zone and the Sapphire Tectonic Block, p. 25-31, in R.B. Chase and D.W. Hyndman, Mylonite detachment zone, eastern flank of Idaho batholith: Geol. Soc. America, Rocky Mtn. Sec. 30th Ann. Mtg. Field guide No. 1.
- _____, 1980, Bitterroot dome - Sapphire tectonic block, an example of a plutonic-core gneiss-dome complex with its detached suprastructure: Geol. Soc. America Memoir 153, p. 427-443.
- _____, Talbot, J.L. and Chase, R.B., 1975, Boulder batholith: A result of emplacement of a block detached from the Idaho batholith infrastructure?: Geology, v. 3, p. 401-404.
- _____, and Williams, L.D., 1977, The Bitterroot lobe of the Idaho batholith: Northwest Geol., v. 6-1, Idaho batholith symposium papers, p. 1-16.
- Jens, J.C., 1974, A layered ultramafic intrusion near Lolo Pass, Idaho: Northwest Geology, v. 3, p. 38-46.
- Johnson, M.R.W., 1967, Mylonite zones and mylonite banding: Nature, v. 213, p. 246-247.
- Langton, C.M., 1935, Geology of the northeastern part of the Idaho batholith and adjacent region in Montana: Jour. Geology, v. 43, p. 27-60.
- Larson, E.S., Jr. and Schmidt, R.G., 1958, A reconnaissance of the Idaho batholith and comparison with the Southern California batholith: U.S. Geol. Survey Bull. 1070-A, p. 1-32.
- Leischner, L.M., 1959, Border zone petrology of the Idaho batholith in vicinity of Lolo Hot Springs, Montana: Unpubl. M.A. thesis, University of Montana, 76 p.
- Lelek, J.J., 1979, The Skalkaho Pyroxenite-Syenite complex east of Hamilton, Montana, and the role of magma immiscibility in its formation: Unpubl. M.S. thesis, University of Montana, 130 p.

- Lindgren, W., 1904, A geological reconnaissance across the Bitterroot Range and Clearwater Mountains in Montana and Idaho: U.S. Geol. Survey Prof. Paper 27, 123 p.
- Mitra, G., 1978, Deformation zones and mylonites: the mechanical processes involved in the deformation of crystalline basement rocks: Amer. Jour. Science, v. 278, p. 1057-1084.
- Nold, J.L., 1974, Geology of the northeast border zone of the Idaho batholith, Montana and Idaho: Northwest Geology, v. 3, p. 47-52.
- Paterson, M.S., and Weiss, L.E., 1961, Symmetry concepts in the structural analysis of deformed rocks: Geol. Soc. America Bull. v. 72, p. 841-871.
- Ross, C.P., 1952, The eastern front of the Bitterroot Range, Montana: U.S. Geol. Survey Bull. 974-E, p. 135-175.
- Snoke, A.W., 1980, Transition from infrastructure to suprastructure in the northern Ruby Mountains, Nevada: Geol. Soc. America Memoir 153, p. 287-333.
- Streckeisen, A., 1976, To each plutonic rock its proper name: Earth-Science Reviews, v. 12, p. 1-33.
- Turner, F.J. and Weiss, L.E., 1963, Structural analysis of metamorphic tectonites: New York, McGraw-Hill Book Co., Inc., 545 p.
- White, B.G., 1969, Structural analysis of a small area in the northeast border zone of the Idaho batholith, Idaho: Unpubl. M.S. thesis, University of Montana, 53 p.
- Wehrenberg, J.P., 1972, Geology of the Lolo Peak area, northern Bitterroot Range, Montana: Northwest Geology, v. 1, p. 25-32.
- Williams, R.D., 1975, Structural and metamorphic geology of the Bass Lake area, northern Bitterroot Range: Unpubl. M.S. thesis, University of Montana, 53 p.

Appendix I

Individual thin section analyses, NM1 - nonmylonitic interior, WMZ = weakly mylonitic zone, SMZ = strongly mylonitic zone, SMZ_{bm} = black mylonite, SMZ_{wm} = white mylonite, SMZ_{bd} = black dike

Sample #	Zone	Plagioclase	K-feldspar	Quartz	Biotite	Muscovite	Myrmecite
BL-3	NM1	28	35	25	5	5	1
BL-4	NM1	41	29	24	4	2	2
B1-5a	NM1	40	20	32	5	3	1
C-10b	NM1	35	25	30	6	1	3
R1-1	NM1	38	27	28	5	2	1
R1-2	NM1	35	25	31	7	1	1
R1-3	NM1	37	33	21	7	1	1
R1-5a	NM1	40	29	25	4	1	1
R1-8	NM1	40	25	25	5	1	2
C-11b	WMZ	50	5	38	5	2	4
RL-10a	WMZ	33	29	27	5	2	3
RL-12a	WMZ	35	25	27	5	2	5
RL-13a	WMZ	34	34	20	4	1	5
RL-13b	WMZ	34	34	20	4	1	5
RL-15a	WMZ	38	25	30	3	1	1
RL-17a	WMZ	31	35	25	3	1	4
RL-19a	WMZ	32	32	25	5	1	3
RL-19b	WMZ	32	32	25	5	1	3
RL-20	WMZ	34	30	27	4	1	3
RL-21	WMZ	27	32	25	6	3	5
C-1a	SMZ	40	29	20	5	4	1
C-2a	SMZ _{bm}	40	32	20	6	tr	1
C-4a	SMZ	25	29	30	6	6	2
C-46	SMZ	32	31	25	5	3	2
C-9a	SMZ _{bm}	40	10	30	2	10	1
GS-1a	SMZ _{bm}	55	10	25	7	2	1
GS-1b	SMZ _{bm}	55	10	25	7	2	1
GS-3b	SMZ	33	25	30	5	2	3
GS-4a	SMZ	30	34	25	2	6	3
GS-11a	SMZ	35	28	26	4	2	4
RL-25a	SMZ	29	25	30	2	2	8
RL-26a	SMZ _{bm}	30	39	25	2	1	2
RL-26b	SMZ _{bm}	30	39	25	2	1	2
RL-27a	SMZ _{bm}	29	29	27	5	2	5
RL-27b	SMZ _{bm}	29	29	27	5	2	5
RL-29a	SMZ _{bm}	32	27	30	3	1	5
RL-30a	SMZ _{wm}	31	38	25	1	0	3
	SMZ _{bd}	66	0	20	12	0	0

Appendix I (continued)

<u>Sample #</u>	<u>Zone</u>	<u>Plagioclase</u>	<u>K- feldspar</u>	<u>Quartz</u>	<u>Biotite</u>	<u>Musco- vite</u>	<u>Myrme- kite</u>
RL-30b	SMZ _{wm}	31	38	25	1	0	3
RL-A	SMZ	32	36	23	4	1	3
RL-B	SMZ	32	36	23	4	1	3

Accessory minerals common to all units: chlorite, opaque minerals, apatite, zircon, sericite, rutile and sphene. Sillimanite occurs in several samples in NM1 and one sample in WMZ.

Appendix 2

Table 2. Chemical analyses and molecular norms of samples from nonmylonitic and mylonitic samples of the Idaho batholith. (Adapted from Chase, 1973)

	NMI Samples									WMZ Samples		SMZ Samples
SiO ₂	68.6	67.4	68.3	69.1	73.5	69.0	67.3	63.3	63.3	70.2	70.6	67.7
TiO ₂	0.2	0.2	0.2	0.2	0.2	0.2	0.4	0.4	0.6	0.2	0.2	0.2
Al ₂ O ₃	15.3	14.4	14.8	14.8	16.1	14.8	15.2	16.6	16.7	15.3	14.4	15.2
Fe ₂ O ₃	2.4	2.1	2.0	1.3	1.9	2.2	2.8	4.2	5.3	1.6	1.7	2.0
MgO	0.8	0.8	1.0	0.6	0.7	0.7	1.5	1.7	1.5	0.9	0.9	1.5
CaO	1.7	2.0	2.0	1.5	1.8	1.7	3.2	3.5	2.8	1.7	1.6	1.8
Na ₂ O	4.7	4.8	4.7	3.9	4.7	4.1	4.4	5.4	4.7	3.7	4.6	3.5
K ₂ O	3.9	3.2	3.5	5.1	4.6	4.5	1.7	1.6	4.3	4.1	4.1	3.6
H ₂ O ⁺	<u>0.3</u>	<u>0.5</u>	<u>0.3</u>	<u>0.2</u>	<u>0.3</u>	<u>0.2</u>	<u>0.6</u>	<u>0.3</u>	<u>0.3</u>	<u>0.2</u>	<u>0.3</u>	<u>0.5</u>
TOTAL	97.9	96.4	96.8	96.7	103.8	97.4	97.1	97.0	99.5	97.9	98.4	96.0
Molecular norms												
q	20.3	21.1	21.2	21.6	21.1	20.8	25.3	15.4	11.0	27.0	22.6	26.8
or	23.5	26.0	21.0	31.5	26.0	28.0	10.5	9.5	25.5	25.0	24.5	22.5
ab	43.5	41.0	43.5	36.5	41.0	39.0	41.0	49.5	42.5	33.5	42.0	33.0
an	8.5	8.5	9.5	7.5	8.5	8.5	16.0	17.0	11.8	8.5	6.8	9.0
c	0.3	0.2	-	0.1	0.2	-	0.5	-	-	2.1	-	2.7
wo	-	-	0.4	-	-	-	-	0.4	0.8	-	0.4	-
en	2.2	1.8	2.8	1.8	1.8	2.0	4.4	5.0	4.2	2.6	2.4	4.4
fs	iron calculated as Fe ₂ O ₃											
il*	0.2	0.2	0.4	0.2	0.2	0.4	0.4	0.6	1.0	0.2	0.2	0.2
mt	iron calculated as Fe ₂ O ₃											
hm	<u>1.6</u>	<u>1.2</u>	<u>1.2</u>	<u>0.8</u>	<u>1.2</u>	<u>1.4</u>	<u>1.8</u>	<u>2.5</u>	<u>3.2</u>	<u>1.0</u>	<u>1.1</u>	<u>1.4</u>
TOTAL	100.1	100.0	100.0	100.0	100.0	100.1	99.9	99.9	100.0	99.9	100.0	100.0

*Sufficient Fe₂O₃ recalculated as FeO to make ilmenite.

Appendix 2 (cont.)

Variation diagram of Idaho batholith and mylonitic equivalents.
 Circles - nonmylonitic interior; triangles - weakly mylonitic zone;
 squares - strongly mylonitic zone; crosses - Idaho batholith analyses;
 from Larson and Schmidt (19548, Fig. 2, where iron is analyzed as FeO).
 Curves of best visual fit drawn through analyses of rocks from study area.
 (Adapted from Chase, 1973)

